

A Computational Model of the High Flux Isotope Reactor for the Calculation of Cold Source, Beam Tube, and Guide Hall Nuclear Parameters

Douglas E. Peplow



DOCUMENT AVAILABILITY

Reports produced after January 1, 1996, are generally available free via the U.S. Department of Energy (DOE) Information Bridge:

Web site: <http://www.osti.gov/bridge>

Reports produced before January 1, 1996, may be purchased by members of the public from the following source:

National Technical Information Service
5285 Port Royal Road
Springfield, VA 22161
Telephone: 703-605-6000 (1-800-553-6847)
TDD: 703-487-4639
Fax: 703-605-6900
E-mail: info@ntis.fedworld.gov
Web site: <http://www.ntis.gov/support/ordernowabout.htm>

Reports are available to DOE employees, DOE contractors, Energy Technology Data Exchange (ETDE) representatives, and International Nuclear Information System (INIS) representatives from the following source:

Office of Scientific and Technical Information
P.O. Box 62
Oak Ridge, TN 37831
Telephone: 865-576-8401
Fax: 865-576-5728
E-mail: reports@adonis.osti.gov
Web site: <http://www.osti.gov/contact.html>

This report was prepared as an account of work sponsored by an agency of the United States Government. Neither the United States government nor any agency thereof, nor any of their employees, makes any warranty, express or implied, or assumes any legal liability or responsibility for the accuracy, completeness, or usefulness of any information, apparatus, product, or process disclosed, or represents that its use would not infringe privately owned rights. Reference herein to any specific commercial product, process, or service by trade name, trademark, manufacturer, or otherwise, does not necessarily constitute or imply its endorsement, recommendation, or favoring by the United States Government or any agency thereof. The views and opinions of authors expressed herein do not necessarily state or reflect those of the United States Government or any agency thereof.

Nuclear Science and Technology Division

**A COMPUTATIONAL MODEL OF THE HIGH FLUX ISOTOPE
REACTOR FOR THE CALCULATION OF COLD SOURCE, BEAM
TUBE, AND GUIDE HALL NUCLEAR PARAMETERS**

Douglas E. Peplow

Date Published: November 2004

Prepared by
OAK RIDGE NATIONAL LABORATORY
P.O. Box 2008
Oak Ridge, Tennessee 37831-6283
managed by
UT-BATTELLE, LLC
for the
U.S. DEPARTMENT OF ENERGY
under contract DE-AC05-00OR22725

CONTENTS

	Page
LIST OF FIGURES	v
LIST OF TABLES	vii
ACKNOWLEDGMENTS	ix
ABSTRACT	1
1. INTRODUCTION	1
2. CONTENTS OF THE MODEL	3
2.1 TARGET REGION	3
2.2 FUEL REGION.....	3
2.3 CONTROL ELEMENTS	16
2.4 BERYLLIUM REFLECTOR.....	16
2.5 HORIZONTAL BEAM TUBES 1, 2, AND 3	16
2.6 HORIZONTAL BEAM TUBE 4 AND COLD SOURCE	23
2.7 REACTOR VESSEL AND CONCRETE SHIELDING.....	23
2.8 DETAILED BEAM TUBE GEOMETRIES	23
2.9 SPECIAL CROSS SECTIONS USED IN HF245	23
3. COMPARISONS TO MEASURED VALUES	29
3.1 TARGET REGION PEAK THERMAL NEUTRON FLUX.....	29
3.2 HYDRAULIC TUBE NEUTRON FLUXES.....	29
3.3 REFLECTOR THERMAL NEUTRON FLUXES.....	33
3.4 MULTIPLICATION FACTOR	34
4. SUMMARY	37
REFERENCES	39
Appendix A. FILES ON THE ACCOMPANYING CD	A-1

LIST OF FIGURES

Figure		Page
1	The target holder assembly.....	4
2	The core region	7
3	The control rods	17
4	The control rod positions in the MCNP model using surface transformations	19
5	The beryllium reflector.....	21
6	Horizontal beam tube 2	22
7	Horizontal beam tube 3	24
8	The cold source moderator inside horizontal beam tube 4	25
9	The pool region	27
10	Total fluxes—ORNL/TM-12831 and the hf2004 model.....	31
11	Thermal fluxes—ORNL/TM-12831 and the hf2004 model.....	31
12	Fast fluxes (>0.1 MeV)—ORNL/TM-12831 and the hf2004 model	32
13	Fast fluxes (>1.0 MeV)—ORNL/TM-12831 and the hf2004 model	32
14	Average fluxes—ORNL/TM-12831 (Table 14) and the hf2004 model.....	33

LIST OF TABLES

Table		Page
1	Comparison between the HF245 model and the new hf2004 model.....	2
2	Target region of the MCNP model.....	5
3	Material codes and volumes for the target regions	5
4	Weight fractions of the stainless steel materials used in the target region.....	5
5	Isotopic weight fractions and densities for water, Al 6061, and Al 1100.....	6
6	Isotopic weight fractions and densities for the curium target rods	6
7	Materials by radial and axial locations in the inner and outer fuel elements (BOC).....	8
8	Materials by radial and axial locations in the inner and outer fuel elements (EOC).....	9
9	Amounts of selected isotopes in the fuel regions of the MCNP model	9
10	Isotopic weight fractions for the inner fuel element materials (BOC)	10
11	Isotopic weight fractions for the outer fuel element materials (BOC)	11
12	Isotopic weight fractions and densities for the inner fuel element materials (EOC)	12
13	Isotopic weight fractions and densities for the outer fuel element materials (EOC)	14
14	Control element dimensions.....	18
15	Isotopic weight fractions and densities for the control elements	18
16	Isotopic weight fractions and densities of the reflector materials	20
17	Isotopic weight fractions and densities for pool, vessel and biological shield materials.....	26
18	Measured and calculated thermal fluxes and saturation activities in the center of the HFIR reactor	30
19	Ratios of the MCNP calculated flux values to the measured flux values in the hydraulic tube for both BOC and EOC	33
20	Values calculated with the MCNP model and Glasgow 2004.....	35
21	Values and one-sigma relative uncertainties for keff calculated with MCNP models.....	35

ACKNOWLEDGMENTS

The author would like to acknowledge the technical reviews of this document that were performed by R. Trenton Primm III and Jeffrey O. Johnson, both of Oak Ridge National Laboratory (ORNL). The author would also like to acknowledge the technical editing of C. C. Southmayd and the document preparation performed by B. J. Smith, both of ORNL. Finally, the author wishes to acknowledge M. B. Farrar, ORNL, for providing programmatic support for this work.

The development of the computational model described in this report was initiated by L. A. Smith (formerly of ORNL, currently at Entergy Services, Inc.) and continued by J. C. Gehin, J. P. Renier, and J. A. Bucholz (all of ORNL).

A COMPUTATIONAL MODEL OF THE HIGH FLUX ISOTOPE REACTOR FOR THE CALCULATION OF COLD SOURCE, BEAM TUBE, AND GUIDE HALL NUCLEAR PARAMETERS

Douglas E. Peplow

ABSTRACT

This report presents a description of the key elements of a computational model of the High Flux Isotope Reactor (HFIR). The model is an input dataset for the Monte Carlo N-Particle (MCNP) computer program. The model, designated hf2004, with auxiliary portions is a simple representation of the HFIR. Neutronics parameters for a particular point in the fuel cycle, with the appropriate fuel materials and vertical settings for the control elements can easily be built using these files. Various validation studies performed using MCNP version 5 show that the model predicts total flux in the core region well and fluxes in the reflector experiment locations to a fair degree. The model includes a representation of a hydrogen cold source that is expected to be installed in 2006. The model was developed to serve as a basis for calculation of nuclear design parameters for the cold source, beam tubes, wave guides, and associated guide hall structures.

1. INTRODUCTION

This report provides documentation and validation of a computational model of the High Flux Isotope Reactor (HFIR) and certain facilities located in that reactor. The model is input to the Monte Carlo N-Particle (MCNP) code (X-5 Monte Carlo Team 2003). Neutron and photon fluxes and flux-related parameters can be calculated with this program. It is anticipated that this model will be used for heating calculations for the cold source (Johnson 2004).

Several individuals contributed to the development of the model, and some results from the model are presented in (Bucholz 2000, Gehin 1996). None of these individuals had sufficient resources to document their models. This document was written to provide a guide to the model, a reference for subsequent calculations expected to be performed, and to validate the model to the extent possible with comparisons of calculated and measured parameters.

Over time, the model has been modified and used for many different types of calculations. Many of these changes have been left in the model as comment statements. Unfortunately, the large number of comment statements, special purpose regions/materials, and descriptive narratives in the model had made the model too long and too complex to be used by others for quick but quality-assured calculations. In addition to performing some simple checks on the geometry and materials, one of the tasks accomplished during the preparation of this report was to reduce the components of the HFIR MCNP model to elements common to all anticipated uses for the model. That is, it is expected that in future uses of the model, the analyst may wish to add detail to the model or even add components. Some of these additions may be retained and documented to create a new "reference" model. Likely, many of these additions would be for special purposes not of interest to other users and the goals of simplicity and ease-of-use would preclude the establishment of a new, reference model.

Simplification of a model received from J. A. Bucholz, Oak Ridge National Laboratory (ORNL), and designated by him as HF245, resulted in a new model, designated by this report as hf2004. Comparisons of HF245 and the new model, hf2004, are shown in Table 1.

Table 1. Comparison between the HF245 model and the new hf2004 model

	HF245	hf2004	
	(EOC) ^a	(BOC) ^b	(EOC)
Size of file (bytes)	1,197,604	153,353	166,814
Length of file (lines)	13998	2141	2324
Geometry cells	1392	668	668
Geometry surfaces	733	614	614
Geometry transformations	107	8	8
Materials	110	51	64
Sources	Many options	0	0
Tallies	8 × 640	0	0

^aEOC = end of cycle

^bBOC = beginning of cycle

Some of the detailed geometries that were replaced with simplified representations and alternative sets of fuel region materials were kept in an auxiliary file called hf2004.aux. These are arranged in modules that match the structure of the hf2004 file. Modules from the auxiliary file can easily be placed into the hf2004 model, depending on modeling needs. However, should an analyst choose to make use of this auxiliary input, it is the responsibility of that analyst to validate the addition. The validation of the hf2004 model that is documented in this report does not extend to uses involving additions from the auxiliary file.

2. CONTENTS OF THE MODEL

The reader is referred to (Binford 1968) for a general description of the HFIR and to (Cheverton 1971) for a discussion of reactor physics and design of the reactor core and reflector. Subsequent discussion in this report is based on the assumption that the reader is familiar with the geometry and material composition of the reactor core, reflector, and central target region.

The intent of this section is to present sufficient information to verify that the MCNP geometric model is an accurate representation of the HFIR at the time of publication of this document. To that end, reference is made to engineering drawings that provide dimensions and configurations of the components of the reactor core and reflector. Images from the hf2004 model have been generated with a Java visualization tool (Sulfredge 2002). Model configurations are easily verified by viewing the following figures. Dimensions were verified by comparing information from the visualization editor or direct visual comparison of the code input to the relevant engineering drawings.

Material compositions (atom densities) were verified by comparison to values contained in Appendix A of (Cheverton 1971). Those changes in HFIR that have occurred since the publication of (Cheverton 1971) are noted subsequently. None of the cells in the hf2004 make use of the TMP or THTME cards; therefore, all of the cross sections are broadened to a temperature of 293 K, except for the hydrogen in the cold source which uses $S(\alpha,\beta)$ thermal scattering data at 20 K. The hf2004 model uses only cross sections that are a part of the standard MCNP distribution. Additional cross sections for special purposes can be used, as discussed in Sect. 2.9.

2.1 TARGET REGION

The target region of the flux trap consists of 37 separate channels surrounded by an aluminum target holder, shown in Fig. 1. The target is internal to the inner fuel element.

The outermost, symmetric, six positions are known as peripheral target positions (PTP). Each PTP location can accommodate seven specimens placed one-atop-the other. These specimens are typically 6 cm in length. The MCNP model does not currently divide the PTP or other channels into axial segments, except for the thermal-hydraulic tube, which has nine axial segments.

One of the remaining 31 positions is a thermal-hydraulic tube that allows specimens to be inserted/removed from the target region while the reactor is operating. The remaining 30 channels contain a typical assortment of different materials, including curium pins, stainless steel experiments, and aluminum dummy rods. Each rod contains cladding as a separate region, and the target materials can easily be changed. Note that the target configuration modeled does not correspond to an actual irradiation but rather represents a collection of typical rods. Characteristics of the target pins contained in the MCNP model are shown in Tables 2–6.

2.2 FUEL REGION

The HFIR core uses two annular sets of curved fuel plates. The inner fuel region is represented in the MCNP model by a set of seven axial layers of eight concentric rings. The outer annulus is modeled with seven axial layers of nine rings (see Fig. 2 and Tables 7 and 8). Each of these 119 fuel regions is assigned a material from one of two material sets—a beginning-of-cycle (BOC) set or an end-of-cycle (EOC) set. These material definitions reflect the changing uranium density as a function of radius and the buildup of neutron absorbers as a function of axial position. Uranium concentration is similar to that given in Appendix A of (Cheverton 1971). The standard model, hf2004, contains atom densities corresponding to what Gehin (1996) determined for BOC

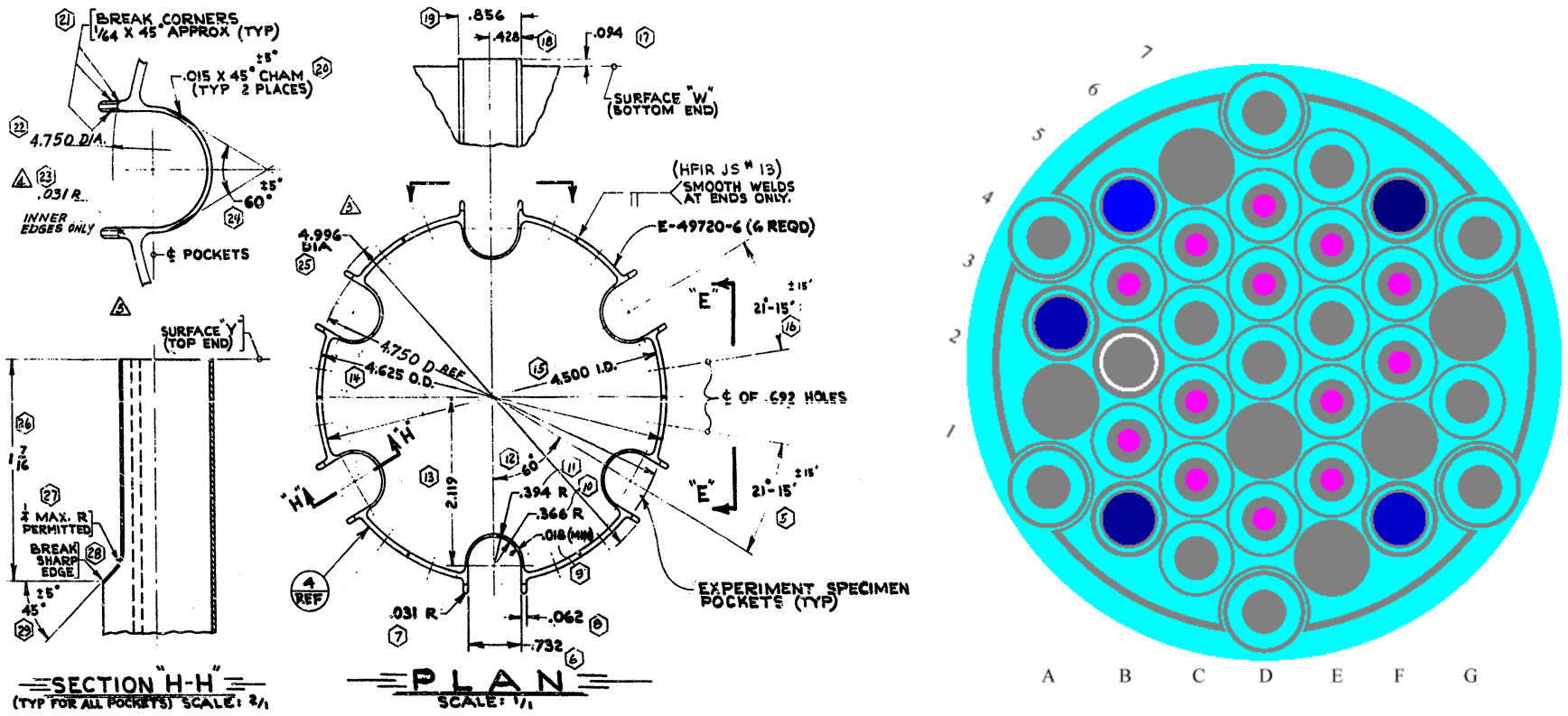


Fig. 1. The target holder assembly. On the left as shown in HFIR drawing E-49722 and on the right from the MCNP model. (Key: gray—aluminum, magenta—curium targets, white—void, light blue—water, dark blues—aluminum with steel.)

Table 2. Target region of the MCNP model

Target	Location
Stainless steel experiments	A-3, B-1, B-5, F-3, F-7
Curium targets	B-2, B-4, C-2, C-3, C-5, D-2, D-5, D-6, E-3, E-4, E-6, F-5, F-6
HT tube	B-3
PTP	A-1, A-4, D-1, D-7, G-4, G-7
Shrouded aluminum dummy	C-1, C-4, D-4, E-5, E-7, G-5
Solid aluminum dummy	A-2, C-6, D-3, E-2, F-4, G-6

Table 3. Material codes and volumes for the target regions

	Material code				Volume (cm ³)			
	Target	Tube	Clad	Shroud	Target	Tube	Clad	Shroud
Stainless steel experiment	51x ^a	20	20	20	51.3182	13.0336	48.2639	37.2563
Curium targets	510	511	20	20	9.7879	6.1716	47.3868	24.7391
HT tube	20	20	20		16.4764	40.1966	39.8852	
PTP 1-6	20		20	20	36.1599		8.3522	31.8966
Shrouded aluminum dummy	20	511	20	20	9.7879	6.1716	47.3868	24.7391
Solid aluminum dummy	20			20	63.3464			95.6087

^aFive different stainless steels, see Table 4.

Table 4. Weight fractions of the stainless steel materials used in the target region

Material code		513	514	515	516	517
Location		B-5	F-3	A-3	B-1	F-7
Stainless		5%	10%	20%	30%	40%
Density^a	g/cm³	-2.960157	-3.220156	-3.740167	-4.260172	-4.780183
	/(b cm)	0.0615650	0.0628639	0.0654619	0.0680598	0.0706578
Library		Weight fractions				
6012	50c C	1.067E-04 ^b	1.961E-04	3.376E-04	4.446E-04	5.284E-04
13027	50c Al	8.666E-01	7.547E-01	5.775E-01	4.437E-01	3.389E-01
24000	50c Cr	2.535E-02	4.661E-02	8.026E-02	1.057E-01	1.256E-01
26000	50c Fe	9.530E-02	1.752E-01	3.017E-01	3.973E-01	4.721E-01
28000	50c Ni	1.268E-02	2.331E-02	4.014E-02	5.285E-02	6.281E-02

^aMCNP uses sign to indicate density units: g/cm³ is negative, /(b cm) is positive.

^bE-04 should be read as 10⁻⁴.

Table 5. Isotopic weight fractions and densities for water, Al 6061, and Al 1100

Material code		1	20	511
		Water	Al 6061	Al 1100
Densities	g/cm³	-1	-2.7	-2.709982
	/(b cm)	0.10031015	0.06032088	0.060324
	g/cm³		-2.16	
	/(b cm)		0.04825671	
Library		Weight fractions		
1001	50c	H	1.119E-01	2.147E-04
8016	50c	O	8.881E-01	
12000	50c	Mg		1.002E-02
13027	50c	Al		9.734E-01
14000	50c	Si		6.011E-03
22000	50c	Ti		7.514E-04
24000	50c	Cr		1.954E-03
25055	50c	Mn		7.514E-04
26000	55c	Fe		3.507E-03
29000	50c	Cu		3.424E-03
				2.500E-04
				2.500E-03
				2.000E-03

Table 6. Isotopic weight fractions and densities for the curium target rods

Material code		510		
Density g/cm³		-3.050287		
/(b cm)		0.050946		
Library		Weight fraction		
8016	50c	O	0.057782	
13027	50c	Al	0.614838	
94240	50c	Pu	0.004962	
95241	50c	Am	0.020968	
95243	50c	Am	0.004929	
96244	50c	Cm	0.082058	
96245	35c	Cm	0.001228	
96246	35c	Cm	0.174151	
96247	35c	Cm	0.005073	
96248	35c	Cm	0.03401	

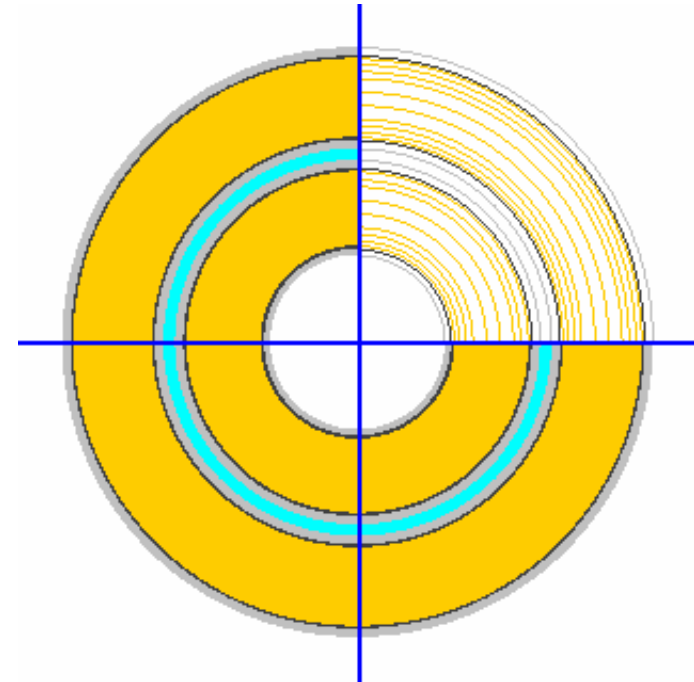
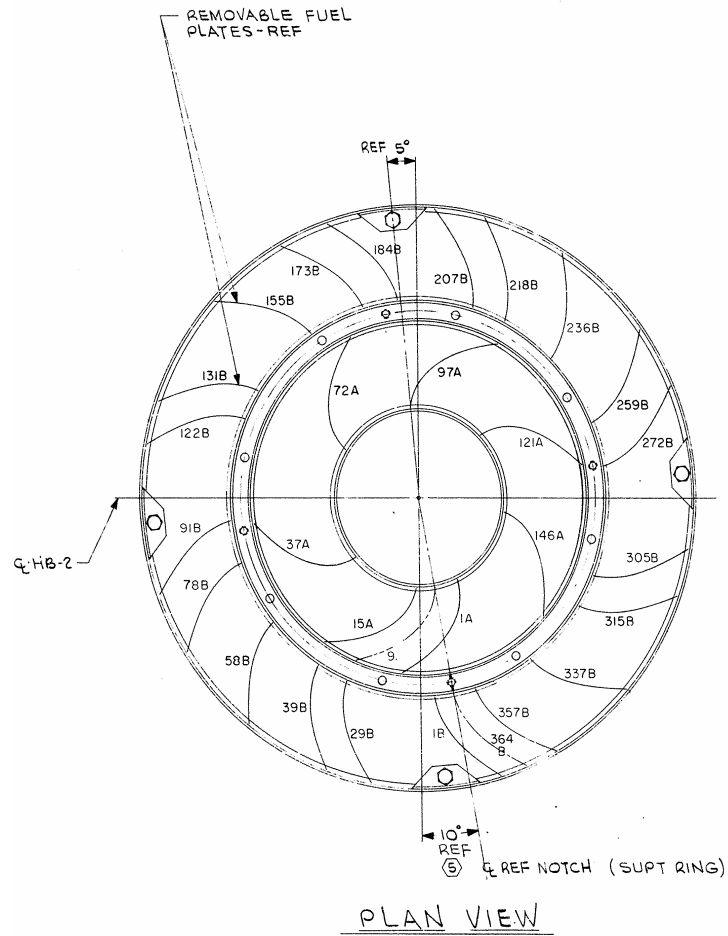


Fig. 2. The core region. Shown on the left from HFIR drawing E-49636 and on the right from the MCNP model. Both the inner and outer fuel annuli are made of concentric rings of slightly different composition, as shown in the upper right-hand portion of the MCNP figure. (Key: yellow—fuel, gray—aluminum, blue—water, dark gray—Al/H₂O mixture.)

Table 7. Materials by radial and axial locations in the inner and outer fuel elements (BOC)

		Axial limits (cm)								
		25.4	19	11	3	-3	-11	-19	-25.4	
		19	11	3	-3	-11	-19	-25.4		
Radial limits (cm)	Inner	7.14121	7.5	201	201	201	201	201	201	201
		7.5	8	202	202	202	202	202	202	202
		8	8.5	203	203	203	203	203	203	203
		8.5	9.5	204	204	204	204	204	204	204
		9.5	10.5	205	205	205	205	205	205	205
		10.5	11.5	206	206	206	206	206	206	206
		11.5	12	207	207	207	207	207	207	207
		12	12.5984	208	208	208	208	208	208	208
	Outer	15.12951	15.5	301	301	301	301	301	301	301
		15.5	16	302	302	302	302	302	302	302
		16	16.5	303	303	303	303	303	303	303
		16.5	17.5	304	304	304	304	304	304	304
		17.5	18.5	305	305	305	305	305	305	305
		18.5	19.5	306	306	306	306	306	306	306
		19.5	20	307	307	307	307	307	307	307
		20	20.5	308	308	308	308	308	308	308
20.5	20.93341	309	309	309	309	309	309	309		

Table 8. Materials by radial and axial locations in the inner and outer fuel elements (EOC)

		Axial limits (cm)								
		25.4 19	19 13	13 3	3 -3	-3 -13	-13 -19	-19 -25.4		
Radial limits (cm)	Inner	7.14121	7.5	201	201	205	205	205	209	209
		7.5	8	201	201	205	205	205	209	209
		8	8.5	201	201	205	205	205	209	209
		8.5	9.5	202	202	206	206	206	210	210
		9.5	10.5	203	203	207	207	207	211	211
		10.5	11.5	203	203	207	207	207	211	211
		11.5	12	204	204	208	208	208	212	212
		12	12.5984	204	204	208	208	208	212	212
	Outer	15.12951	15.5	301	301	307	307	307	313	313
		15.5	16	302	302	308	308	308	314	314
		16	16.5	302	302	308	308	308	314	314
		16.5	17.5	303	303	309	309	309	315	315
		17.5	18.5	303	303	309	309	309	315	315
		18.5	19.5	304	304	310	310	310	316	316
		19.5	20	305	305	311	311	311	317	317
		20	20.5	305	305	311	311	311	317	317
20.5	20.93341	306	306	312	312	312	318	318		

and EOC using VENTURE. Both the BOC regions and materials and the EOC regions and materials are listed in the auxiliary file, hf2004.aux, and can be placed in the standard model, hf2004. The model hf2004, if executed without any modification, will model BOC conditions.

Boron and ^{235}U masses were computed from the MCNP model and compared to values published in (Cheverton 1971). The ^{10}B content of the inner element in the BOC MCNP model is 2.799 g; Cheverton reports a value of 2.8 g ^{10}B . The ^{235}U content of the inner and outer elements, combined, in the MCNP model is 9.366 kg; Cheverton reports a value of 9.4 kg. Values for these isotopes are shown in Table 9. Weight fractions for each isotope in each fuel material are shown in Tables 10–13. The small amount of boron in the outer fuel region for the EOC core is to account for fission products other than xenon and samarium.*

Table 9. Amounts of selected isotopes in the fuel regions of the MCNP model

	BOC			EOC		
	^{10}B (g)	^{11}B (g)	^{235}U (g)	^{10}B (g)	^{11}B (g)	^{235}U (g)
Inner	2.799	12.47	2593	0.711	12.03	1504
Outer	0	0	6773	1.156	0	4907

*Gehin (1996) derived the boron concentrations by using a VENTURE model and the EOC number densities/cross sections for the fission products not represented in the MCNP model and computed the total absorption rate. This total absorption rate was used to compute the effective boron number density that results in the same absorption rate. This is performed not for only the thermal absorption rate, but the total. This was applied to each spatial region in the model for both the inner and outer elements.

Table 10. Isotopic weight fractions for the inner fuel element materials (BOC)

Materia			201	202	203	204	205	206	207	208
l code										
Density, g/cm³			-1.918577	-1.933521	-1.950707	-1.974920	-1.998506	-2.000651	-1.988310	-1.973369
/(b cm)			0.0800804	0.0800839	0.080088	0.0800937	0.0800993	0.0800998	0.0800968	0.0800933
1001	50c	H	2.900E-02	2.877E-02	2.852E-02	2.817E-02	2.784E-02	2.781E-02	2.798E-02	2.819E-02
5010	50c	B	1.769E-04	1.526E-04	1.252E-04	8.739E-05	5.142E-05	4.819E-05	6.686E-05	8.978E-05
5011	50c	B	7.879E-04	6.799E-04	5.577E-04	3.892E-04	2.290E-04	2.146E-04	2.978E-04	3.999E-04
8016	50c	O	2.378E-01	2.377E-01	2.377E-01	2.376E-01	2.375E-01	2.375E-01	2.375E-01	2.376E-01
12000	50c	Mg	2.815E-03	2.793E-03	2.768E-03	2.734E-03	2.702E-03	2.699E-03	2.716E-03	2.736E-03
13027	50c	Al	6.772E-01	6.683E-01	6.581E-01	6.442E-01	6.309E-01	6.297E-01	6.366E-01	6.450E-01
14000	50c	Si	2.705E-03	2.675E-03	2.641E-03	2.594E-03	2.549E-03	2.545E-03	2.568E-03	2.597E-03
22000	50c	Ti	2.111E-04	2.095E-04	2.076E-04	2.051E-04	2.027E-04	2.024E-04	2.037E-04	2.052E-04
24000	50c	Cr	5.488E-04	5.446E-04	5.398E-04	5.332E-04	5.269E-04	5.263E-04	5.296E-04	5.336E-04
25055	50c	Mn	3.127E-04	3.094E-04	3.056E-04	3.004E-04	2.954E-04	2.949E-04	2.975E-04	3.007E-04
26000	50c	Fe	2.002E-03	1.977E-03	1.949E-03	1.910E-03	1.873E-03	1.870E-03	1.889E-03	1.912E-03
29000	50c	Cu	1.528E-03	1.511E-03	1.492E-03	1.465E-03	1.440E-03	1.438E-03	1.451E-03	1.467E-03
92234	51c	U	4.471E-04	5.413E-04	6.479E-04	7.950E-04	9.348E-04	9.473E-04	8.747E-04	7.856E-04
92235	50c	U	4.185E-02	5.067E-02	6.064E-02	7.441E-02	8.749E-02	8.867E-02	8.188E-02	7.354E-02
92236	50c	U	1.804E-04	2.184E-04	2.614E-04	3.207E-04	3.771E-04	3.822E-04	3.529E-04	3.170E-04
92238	50c	U	2.456E-03	2.973E-03	3.559E-03	4.366E-03	5.134E-03	5.203E-03	4.805E-03	4.315E-03

Table 11. Isotopic weight fractions for the outer fuel element materials (BOC)

Material code			301	302	303	304	305	306	307	308	309
Density, g/cm³			-1.989230	-2.017151	-2.046917	-2.073935	-2.065654	-2.025163	-1.986715	-1.961308	-1.938214
/(b cm)			0.0800583	0.0800895	0.0801228	0.080153	0.0801437	0.0800985	0.0800555	0.0800271	0.0800013
1001	50c	H	2.797E-02	2.758E-02	2.718E-02	2.683E-02	2.693E-02	2.747E-02	2.800E-02	2.837E-02	2.870E-02
8016	50c	O	2.376E-01	2.374E-01	2.373E-01	2.371E-01	2.372E-01	2.374E-01	2.376E-01	2.377E-01	2.379E-01
12000	50c	Mg	2.715E-03	2.677E-03	2.638E-03	2.604E-03	2.614E-03	2.666E-03	2.718E-03	2.753E-03	2.786E-03
13027	50c	Al	6.359E-01	6.205E-01	6.046E-01	5.906E-01	5.948E-01	6.162E-01	6.373E-01	6.517E-01	6.651E-01
14000	50c	Si	2.566E-03	2.514E-03	2.460E-03	2.412E-03	2.427E-03	2.499E-03	2.570E-03	2.619E-03	2.665E-03
22000	50c	Ti	2.036E-04	2.008E-04	1.979E-04	1.953E-04	1.961E-04	2.000E-04	2.039E-04	2.065E-04	2.090E-04
24000	50c	Cr	5.294E-04	5.220E-04	5.144E-04	5.077E-04	5.098E-04	5.200E-04	5.300E-04	5.369E-04	5.433E-04
25055	50c	Mn	2.973E-04	2.915E-04	2.856E-04	2.803E-04	2.819E-04	2.899E-04	2.978E-04	3.032E-04	3.083E-04
26000	50c	Fe	1.887E-03	1.844E-03	1.800E-03	1.761E-03	1.773E-03	1.832E-03	1.891E-03	1.931E-03	1.968E-03
29000	50c	Cu	1.450E-03	1.421E-03	1.390E-03	1.363E-03	1.372E-03	1.412E-03	1.452E-03	1.480E-03	1.505E-03
92234	51c	U	8.846E-04	1.045E-03	1.210E-03	1.357E-03	1.312E-03	1.090E-03	8.700E-04	7.201E-04	5.805E-04
92235	50c	U	8.280E-02	9.777E-02	1.133E-01	1.270E-01	1.228E-01	1.020E-01	8.143E-02	6.740E-02	5.433E-02
92236	50c	U	3.569E-04	4.214E-04	4.883E-04	5.473E-04	5.294E-04	4.396E-04	3.510E-04	2.905E-04	2.342E-04
92238	50c	U	4.859E-03	5.737E-03	6.647E-03	7.451E-03	7.207E-03	5.985E-03	4.778E-03	3.955E-03	3.188E-03

Table 12. Isotopic weight fractions and densities for the inner fuel element materials (EOC)

Material	code		201	202	203	204	205	206
Density,	g/cm³		-1.8208658	-1.9237707	-1.984652	-1.9357706	-1.8092748	-1.9094327
	/(b cm)		0.0774938	0.078971	0.0798318	0.079134	0.077464	0.0789341
1001	50c	H	3.004E-02	2.844E-02	2.756E-02	2.826E-02	3.024E-02	2.865E-02
5010	50c	B	1.873E-05	2.418E-05	2.376E-05	2.436E-05	1.810E-05	2.241E-05
5011	50c	B	6.824E-04	3.889E-04	2.321E-04	3.586E-04	6.868E-04	3.918E-04
6012	50c	C	2.319E-04	1.321E-04	7.887E-05	1.219E-04	2.334E-04	1.331E-04
8016	50c	O	2.495E-01	2.407E-01	2.359E-01	2.397E-01	2.511E-01	2.425E-01
12000	50c	Mg	5.466E-03	5.374E-03	5.322E-03	5.363E-03	5.501E-03	5.414E-03
13027	50c	Al	6.604E-01	6.493E-01	6.430E-01	6.479E-01	6.646E-01	6.541E-01
14000	50c	Si	2.733E-03	2.687E-03	2.661E-03	2.681E-03	2.750E-03	2.707E-03
22000	50c	Ti	1.024E-03	1.007E-03	9.975E-04	1.005E-03	1.031E-03	1.015E-03
24000	50c	Cr	2.391E-03	2.351E-03	2.328E-03	2.346E-03	2.407E-03	2.369E-03
25055	50c	Mn	1.025E-03	1.008E-03	9.979E-04	1.005E-03	1.031E-03	1.015E-03
26000	50c	Fe	4.783E-03	4.702E-03	4.657E-03	4.692E-03	4.813E-03	4.738E-03
29000	50c	Cu	2.733E-03	2.687E-03	2.661E-03	2.681E-03	2.751E-03	2.707E-03
54135	50c	Xe	2.105E-07	3.616E-07	4.563E-07	3.858E-07	1.626E-07	3.051E-07
62149	50c	Sm	1.801E-06	2.973E-06	3.748E-06	3.231E-06	1.513E-06	2.671E-06
92234	51c	U	5.071E-04	7.107E-04	8.201E-04	7.341E-04	4.667E-04	6.648E-04
92235	50c	U	3.051E-02	5.107E-02	6.267E-02	5.366E-02	2.311E-02	4.244E-02
92236	50c	U	4.528E-03	4.805E-03	4.843E-03	4.737E-03	5.725E-03	6.333E-03
92238	50c	U	3.222E-03	4.369E-03	4.981E-03	4.490E-03	3.176E-03	4.313E-03
93237	50c	Np	1.303E-04	1.327E-04	1.327E-04	1.297E-04	2.394E-04	2.526E-04
93238	35c	Np	3.387E-06	2.886E-06	2.623E-06	2.664E-06	8.402E-06	7.620E-06
94239	55c	Pu	5.972E-05	9.270E-05	1.109E-04	9.565E-05	6.965E-05	1.141E-04
94240	50c	Pu	1.121E-05	1.267E-05	1.279E-05	1.198E-05	1.733E-05	2.104E-05
94241	50c	Pu	4.217E-06	4.751E-06	4.794E-06	4.470E-06	8.609E-06	1.076E-05

Table 12. (continued)

Material code			207	208	209	210	211	212
Density, g/cm ³			-1.9697868	-1.9217117	-1.8217173	-1.9248273	-1.9858171	-1.9369726
/(b cm)			0.0797936	0.0790977	0.077496	0.0789738	0.0798348	0.0791371
1001	50c	H	2.777E-02	2.847E-02	3.003E-02	2.842E-02	2.755E-02	2.824E-02
5010	50c	B	2.335E-05	2.267E-05	1.898E-05	2.453E-05	2.395E-05	2.475E-05
5011	50c	B	2.339E-04	3.612E-04	6.821E-04	3.886E-04	2.320E-04	3.584E-04
6012	50c	C	7.947E-05	1.227E-04	2.318E-04	1.321E-04	7.882E-05	1.218E-04
8016	50c	O	2.377E-01	2.415E-01	2.494E-01	2.406E-01	2.358E-01	2.396E-01
12000	50c	Mg	5.362E-03	5.402E-03	5.463E-03	5.371E-03	5.319E-03	5.359E-03
13027	50c	Al	6.478E-01	6.526E-01	6.600E-01	6.489E-01	6.426E-01	6.475E-01
14000	50c	Si	2.681E-03	2.701E-03	2.732E-03	2.686E-03	2.660E-03	2.680E-03
22000	50c	Ti	1.005E-03	1.012E-03	1.024E-03	1.007E-03	9.969E-04	1.004E-03
24000	50c	Cr	2.346E-03	2.363E-03	2.390E-03	2.350E-03	2.327E-03	2.345E-03
25055	50c	Mn	1.005E-03	1.013E-03	1.024E-03	1.007E-03	9.973E-04	1.005E-03
26000	50c	Fe	4.692E-03	4.727E-03	4.780E-03	4.700E-03	4.654E-03	4.689E-03
29000	50c	Cu	2.681E-03	2.701E-03	2.732E-03	2.686E-03	2.660E-03	2.680E-03
54135	50c	Xe	3.994E-07	3.315E-07	2.143E-07	3.663E-07	4.618E-07	3.912E-07
62149	50c	Sm	3.491E-06	2.995E-06	1.811E-06	2.980E-06	3.750E-06	3.234E-06
92234	51c	U	7.717E-04	6.884E-04	5.094E-04	7.134E-04	8.230E-04	7.371E-04
92235	50c	U	5.400E-02	4.525E-02	3.105E-02	5.170E-02	6.333E-02	5.437E-02
92236	50c	U	6.451E-03	6.241E-03	4.442E-03	4.697E-03	4.724E-03	4.615E-03
92238	50c	U	4.919E-03	4.433E-03	3.224E-03	4.371E-03	4.983E-03	4.492E-03
93237	50c	Np	2.557E-04	2.496E-04	1.248E-04	1.267E-04	1.263E-04	1.231E-04
93238	35c	Np	7.069E-06	7.121E-06	3.214E-06	2.726E-06	2.468E-06	2.497E-06
94239	55c	Pu	1.412E-04	1.210E-04	5.887E-05	9.106E-05	1.087E-04	9.367E-05
94240	50c	Pu	2.184E-05	2.013E-05	1.082E-05	1.217E-05	1.224E-05	1.144E-05
94241	50c	Pu	1.137E-05	1.043E-05	4.007E-06	4.480E-06	4.494E-06	4.178E-06

Table 13. Isotopic weight fractions and densities for the outer fuel element materials (EOC)

Material code		301	302	303	304	305	306	307	308	309
Density, g/cm³		-1.2306382	-1.3088703	-1.3636594	-1.3033056	-1.2235784	-1.1707837	-1.2157047	-1.2917048	-1.3448566
/(b cm)		0.0633367	0.0640555	0.0645205	0.06393	0.0631685	0.0626612	0.0632988	0.064012	0.0644729
1001	50c H	4.445E-02	4.179E-02	4.012E-02	4.197E-02	4.471E-02	4.672E-02	4.500E-02	4.235E-02	4.068E-02
5010	50c B	2.604E-05	2.705E-05	2.481E-05	2.182E-05	1.880E-05	1.623E-05	3.263E-05	3.490E-05	3.370E-05
8016	50c O	3.789E-01	3.646E-01	3.550E-01	3.644E-01	3.784E-01	3.887E-01	3.835E-01	3.695E-01	3.600E-01
12000	50c Mg	3.760E-03	3.577E-03	3.458E-03	3.583E-03	3.769E-03	3.906E-03	3.806E-03	3.624E-03	3.506E-03
13027	50c Al	4.543E-01	4.321E-01	4.178E-01	4.329E-01	4.554E-01	4.719E-01	4.599E-01	4.379E-01	4.236E-01
14000	50c Si	1.880E-03	1.788E-03	1.729E-03	1.792E-03	1.885E-03	1.953E-03	1.903E-03	1.812E-03	1.753E-03
22000	50c Ti	7.048E-04	6.704E-04	6.481E-04	6.716E-04	7.064E-04	7.321E-04	7.134E-04	6.793E-04	6.571E-04
24000	50c Cr	1.645E-03	1.565E-03	1.513E-03	1.568E-03	1.649E-03	1.709E-03	1.665E-03	1.586E-03	1.534E-03
25055	50c Mn	7.050E-04	6.706E-04	6.484E-04	6.718E-04	7.067E-04	7.324E-04	7.137E-04	6.796E-04	6.574E-04
26000	50c Fe	3.290E-03	3.130E-03	3.026E-03	3.135E-03	3.298E-03	3.418E-03	3.331E-03	3.171E-03	3.068E-03
29000	50c Cu	1.880E-03	1.788E-03	1.729E-03	1.792E-03	1.885E-03	1.953E-03	1.903E-03	1.812E-03	1.753E-03
54135	50c Xe	6.602E-07	9.563E-07	1.195E-06	9.631E-07	6.611E-07	4.639E-07	5.740E-07	8.674E-07	1.094E-06
62149	50c Sm	5.582E-06	7.798E-06	9.412E-06	7.215E-06	4.760E-06	3.258E-06	5.294E-06	7.626E-06	9.306E-06
92234	51c U	1.249E-03	1.608E-03	1.821E-03	1.558E-03	1.174E-03	8.863E-04	1.180E-03	1.531E-03	1.742E-03
92235	50c U	9.152E-02	1.286E-01	1.541E-01	1.302E-01	9.389E-02	6.727E-02	7.786E-02	1.142E-01	1.391E-01
92236	50c U	7.765E-03	7.965E-03	7.249E-03	6.266E-03	5.328E-03	4.585E-03	1.032E-02	1.092E-02	1.046E-02
92238	50c U	7.595E-03	9.606E-03	1.073E-02	9.166E-03	6.938E-03	5.277E-03	7.542E-03	9.553E-03	1.068E-02
93237	50c Np	2.002E-04	1.967E-04	1.668E-04	1.332E-04	1.064E-04	8.691E-05	3.955E-04	4.000E-04	3.602E-04
93238	35c Np	3.859E-06	3.312E-06	2.459E-06	1.999E-06	1.778E-06	1.642E-06	1.062E-05	9.553E-06	7.727E-06
94239	55c Pu	1.531E-04	2.011E-04	2.196E-04	1.716E-04	1.172E-04	8.007E-05	1.997E-04	2.715E-04	3.066E-04
94240	50c Pu	1.808E-05	1.889E-05	1.653E-05	1.356E-05	1.100E-05	8.939E-06	3.130E-05	3.456E-05	3.296E-05
94241	50c Pu	6.381E-06	6.414E-06	5.178E-06	3.887E-06	2.955E-06	2.273E-06	1.562E-05	1.693E-05	1.532E-05

Table 13. (continued)

Material code			310	311	312	313	314	315	316	317	318
Density, g/cm ³			-1.2813406	-1.2002108	-1.1478328	-1.2320512	-1.3104921	-1.3655886	-1.305741	-1.2263374	-1.1737715
/(b cm)			0.0638744	0.0631092	0.062603	0.0633403	0.0640596	0.0645254	0.0639362	0.0631755	0.0626688
1001	50c	H	4.269E-02	4.558E-02	4.766E-02	4.440E-02	4.174E-02	4.006E-02	4.189E-02	4.461E-02	4.661E-02
5010	50c	B	3.194E-05	2.916E-05	2.591E-05	2.545E-05	2.635E-05	2.392E-05	2.068E-05	1.752E-05	1.485E-05
8016	50c	O	3.706E-01	3.858E-01	3.965E-01	3.784E-01	3.642E-01	3.545E-01	3.637E-01	3.776E-01	3.878E-01
12000	50c	Mg	3.645E-03	3.843E-03	3.984E-03	3.756E-03	3.572E-03	3.453E-03	3.577E-03	3.761E-03	3.896E-03
13027	50c	Al	4.403E-01	4.642E-01	4.813E-01	4.538E-01	4.316E-01	4.172E-01	4.321E-01	4.543E-01	4.707E-01
14000	50c	Si	1.822E-03	1.921E-03	1.992E-03	1.878E-03	1.786E-03	1.726E-03	1.788E-03	1.880E-03	1.948E-03
22000	50c	Ti	6.831E-04	7.202E-04	7.467E-04	7.039E-04	6.695E-04	6.472E-04	6.703E-04	7.048E-04	7.302E-04
24000	50c	Cr	1.595E-03	1.681E-03	1.743E-03	1.643E-03	1.563E-03	1.511E-03	1.565E-03	1.645E-03	1.705E-03
25055	50c	Mn	6.834E-04	7.205E-04	7.470E-04	7.042E-04	6.698E-04	6.474E-04	6.706E-04	7.051E-04	7.305E-04
26000	50c	Fe	3.189E-03	3.362E-03	3.486E-03	3.286E-03	3.126E-03	3.021E-03	3.129E-03	3.291E-03	3.409E-03
29000	50c	Cu	1.822E-03	1.921E-03	1.992E-03	1.878E-03	1.786E-03	1.727E-03	1.788E-03	1.880E-03	1.948E-03
54135	50c	Xe	8.281E-07	5.128E-07	3.133E-07	6.697E-07	9.674E-07	1.210E-06	9.814E-07	6.808E-07	4.851E-07
62149	50c	Sm	6.923E-06	4.325E-06	2.735E-06	5.578E-06	7.769E-06	9.351E-06	7.163E-06	4.735E-06	3.262E-06
92234	51c	U	1.483E-03	1.100E-03	8.116E-04	1.253E-03	1.613E-03	1.827E-03	1.565E-03	1.181E-03	8.942E-04
92235	50c	U	1.118E-01	7.259E-02	4.506E-02	9.279E-02	1.300E-01	1.556E-01	1.322E-01	9.635E-02	7.011E-02
92236	50c	U	9.850E-03	9.061E-03	8.210E-03	7.535E-03	7.702E-03	6.940E-03	5.883E-03	4.893E-03	4.111E-03
92238	50c	U	9.154E-03	6.940E-03	5.275E-03	7.596E-03	9.606E-03	1.072E-02	9.163E-03	6.935E-03	5.275E-03
93237	50c	Np	3.221E-04	2.912E-04	2.668E-04	1.883E-04	1.841E-04	1.537E-04	1.191E-04	9.185E-05	7.200E-05
93238	35c	Np	7.292E-06	7.520E-06	7.827E-06	3.579E-06	3.054E-06	2.227E-06	1.747E-06	1.495E-06	1.328E-06
94239	55c	Pu	2.372E-04	1.554E-04	1.013E-04	1.491E-04	1.950E-04	2.112E-04	1.636E-04	1.108E-04	7.502E-05
94240	50c	Pu	2.969E-05	2.549E-05	2.122E-05	1.712E-05	1.776E-05	1.529E-05	1.221E-05	9.664E-06	7.659E-06
94241	50c	Pu	1.296E-05	1.066E-05	8.621E-06	5.886E-06	5.861E-06	4.617E-06	3.336E-06	2.444E-06	1.812E-06

2.3 CONTROL ELEMENTS

Control elements in the HFIR are two concentric annuli that move in opposite directions to allow neutrons to travel from the core to the reflector and back, as shown in Fig. 3. In the axial direction, the control elements consist of three regions, a europium-bearing zone (strongly absorbing of neutrons, aka “black”), a tantalum zone (moderately absorbing region that mitigates flux peaking, aka “gray”), and an aluminum zone (providing flow and structural stability, aka “white”). The control elements change position over the HFIR fuel cycle.

Control element dimensions and materials properties are shown in Tables 14 and 15. Using atom densities from the MCNP model, the europium content of the inner and outer elements combined was found to be 15.13 kg. According to (Sease 1998), the europium content of both control elements combined is 15.34 kg.

The control elements of the HFIR contain small holes throughout to equalize pressures of the coolant material. These holes are not explicitly modeled in the MCNP model, but the different absorbing materials are modeled. The surfaces that describe the axial boundaries of each control element regions are all modified in the MCNP dataset by a simple coordinate transformation card, one for the inner element and one for the outer element. These transformations are easily changed by the user to set the axial position of the control elements to model different stages of the fuel cycle, shown in Fig. 4.

2.4 BERYLLIUM REFLECTOR

The reflector model consists of a set of annular rings of beryllium with trace amounts of lithium and helium that change concentration with radius. These elements are formed in very small amounts in the beryllium during and following operation, but they have high neutron absorption cross sections that have a large influence on k_{eff} calculations. Isotopic weight fractions and densities for the reflector materials are shown in Table 16. The first four materials constitute the inner reflector, with a small annulus of water outside of each one. The last seven materials constitute the outer reflector (permanent reflector) and do not have water gaps. The 198 small coolant channels are not explicitly modeled. A small amount of water is present in the material definitions for the outer reflector region. On the basis of atom densities in the model, water makes up 1.10% of the outer reflector materials by weight. Assuming a beryllium density of 1.85 g/cm³, the water volume is 2.02% of the outer reflector material region volume.

The beryllium reflector contains cut-outs for the experimental facilities, shown in Fig. 5. Twenty-two vertical experimental facilities (VXF, 6 large, 16 small) are modeled in the outer reflector, 12 removable beryllium facilities (8 large, 4 small) in the inner reflector, and 8 control rod access plugs are modeled in the inner reflector. VXF-7 is modeled as an air channel because it contains the pneumatic tube. All of the other VXF facilities are modeled as filled with beryllium or water, though the contents of each of these facilities can easily be changed.

The beryllium regions also contain cut-outs for the four beam tubes and two engineering facilities. Originally, the HFIR contained four engineering facilities. EF3 and EF4 were removed during the early 2000s to accommodate enlargement of the HB2 beam tube. A second pneumatic tube is present in EF2 but is not modeled.

2.5 HORIZONTAL BEAM TUBES 1, 2, AND 3

The model for horizontal beam tube 1 consists of an aluminum container, surrounded by water coolant, placed in an aluminum shell, which is inserted into the beryllium reflector. The thin portion of the container, at the inner tip of the beam tube is modeled explicitly. The innermost region of the beam tube is presently modeled as a void but can be easily changed to any material, such as air or helium. Horizontal beam tube 2 is shown in Fig. 6. It consists of the aluminum

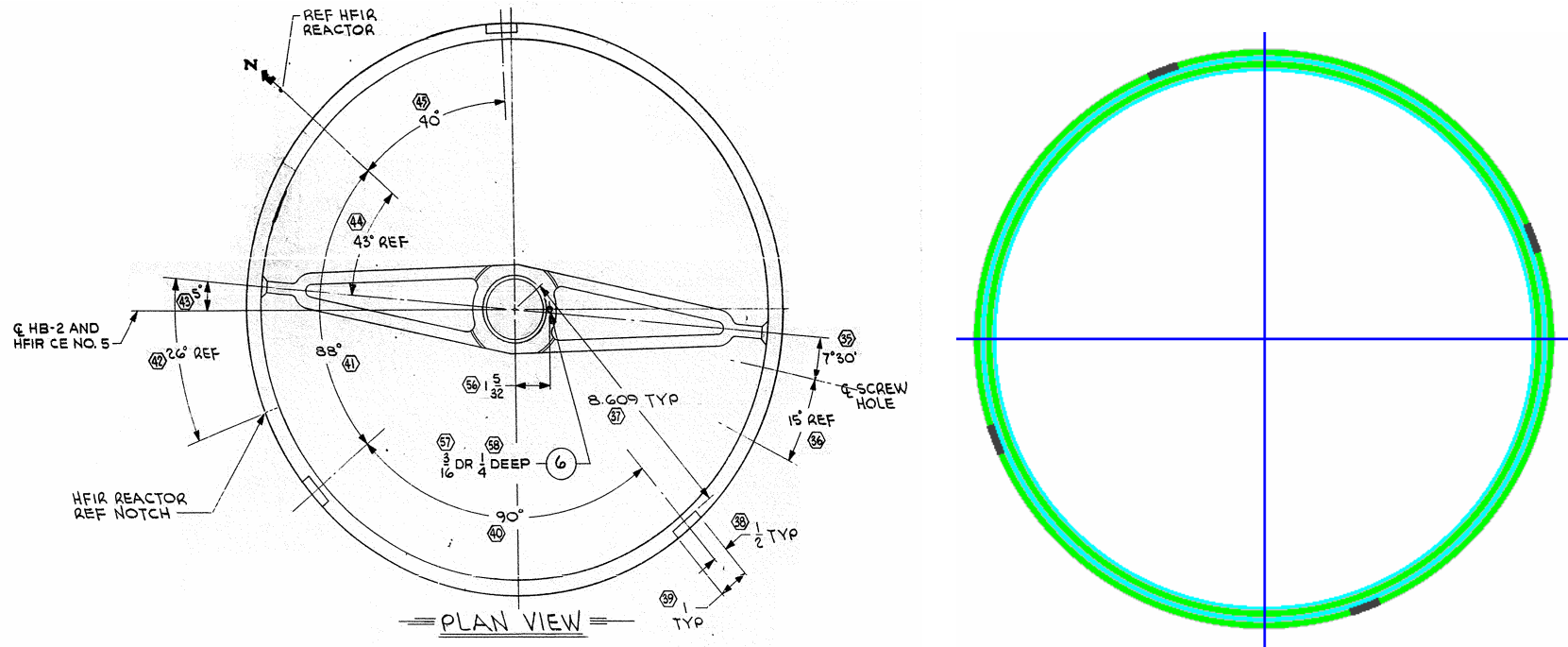


Fig. 3. The control rods. Shown on the left from HFIR drawing E-49882 and on the right from the MCNP model. (Key: green—control element, gray—aluminum, blue—water, dark gray—Al/H₂O mixture.)

Table 14. Control element dimensions

Material		Z_{high} (cm)	Z_{low} (cm)	r_{outer} (cm)	r_{inner} (cm)	Gap	Volume (cm ³)
402	White	111.9188	43.18	22.57997	22.10372	0	4595.528
400	Gray	43.18	30.48	22.57997	22.10372	1.27	787.5737
401	Black	30.48	-25.4	22.57997	22.10372	1.27	3465.324
403	White	-25.4	-61.7538	22.57997	22.10372	0	2430.429
412	White	47.3075	25.4	23.54263	23.06638	1.27	1421.677
410	Black	25.4	-30.48	23.54263	23.06638	1.27	3626.306
411	Gray	-30.48	-43.18	23.54263	23.06638	1.27	824.1604
413	White	-43.18	-120.809	23.54263	23.06638	1.27	5037.68

Table 15. Isotopic weight fractions and densities for the control elements

Material code		Density		1001	8016	13027	63151	63153	73181
		g/cm ³	/(b cm)	50c	50c	50c	50c	50c	51c
				H	O	Al	Eu	Eu	Ta
400	Gray	-7.903	0.06029	6.927E-04	5.497E-03	1.949E-01	0	0	7.989E-01
401	Black	-4.271	0.06132	0	7.888E-02	4.215E-01	2.372E-01	2.624E-01	0
402	White	-2.616	0.06219	2.088E-03	1.657E-02	9.813E-01	0	0	0
403	White	-2.617	0.06215	2.046E-03	1.623E-02	9.817E-01	0	0	0
410	Black	-4.271	0.06132	0	7.888E-02	4.215E-01	2.372E-01	2.624E-01	0
411	Gray	-7.905	0.06028	6.880E-04	5.459E-03	1.949E-01	0	0	7.990E-01
412	White	-2.622	0.06204	1.924E-03	1.527E-02	9.828E-01	0	0	0
413	White	-2.618	0.06215	2.039E-03	1.618E-02	9.818E-01	0	0	0

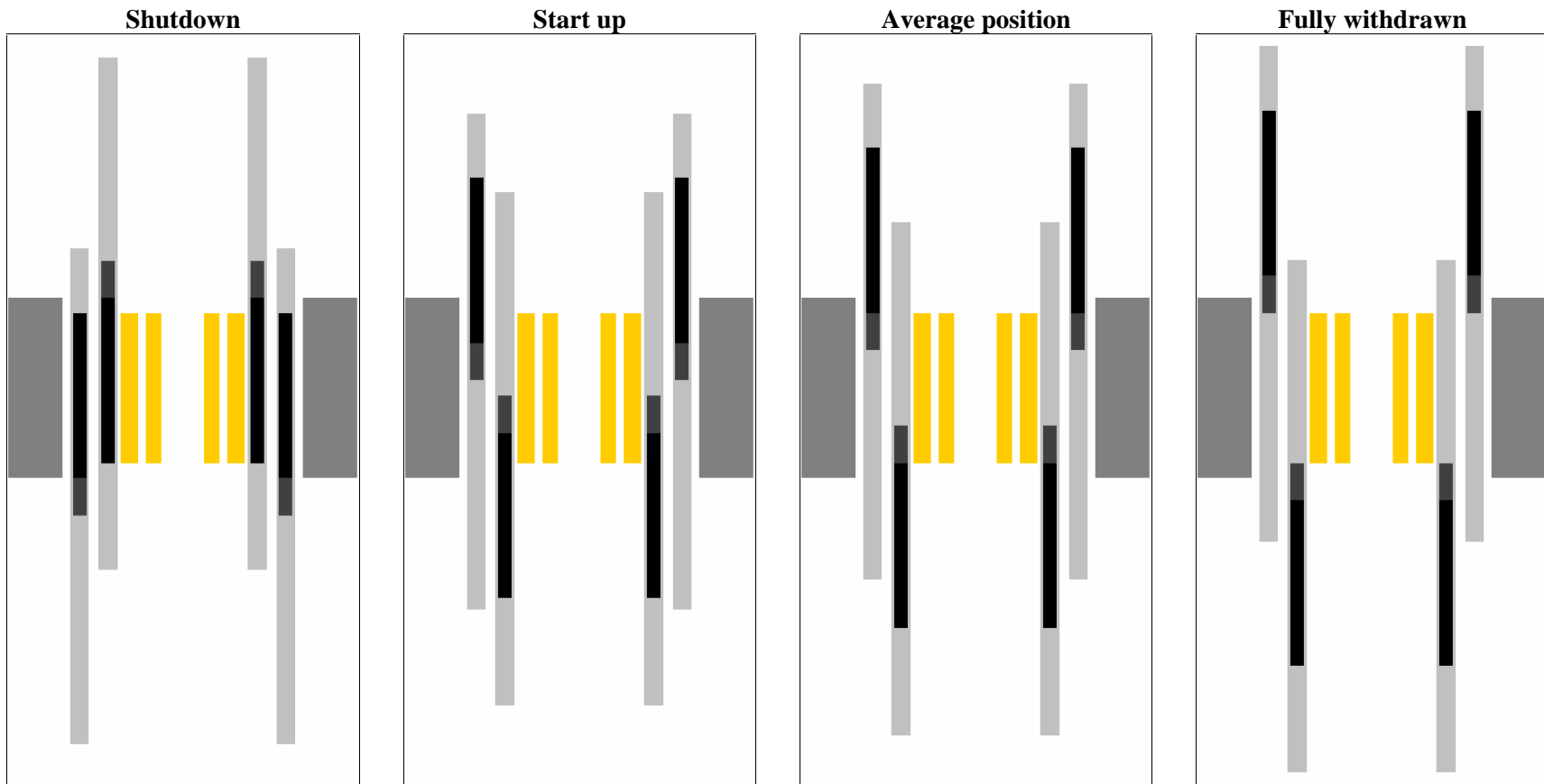


Fig. 4. The control rod positions in the MCNP model using surface transformations. These include (left to right) shutdown, start up, the average position (day 14) and fully withdrawn (EOC). Horizontal dimensions of the control rods have been exaggerated to show details. (Key: yellow—fuel, light gray—aluminum, dark gray—aluminum with tantalum oxide, black—aluminum with europium oxide.)

Table 16. Isotopic weight fractions and densities of the reflector materials

Material code	Density		1001	2003	3006	4009	8016
	g/cm ³	/(b cm)	50c	50c	50c	50c	50c
			H	He	Li	Be	O
101	-1.84978	0.123607	0	1.41E-07	9.58E-06	0.99999	0
102	-1.84978	0.123607	0	8.87E-08	6.01E-06	0.999994	0
103	-1.84979	0.123607	0	4.53E-08	3.07E-06	0.999997	0
104	-1.84979	0.123607	0	2.51E-08	1.70E-06	0.999998	0
105	-1.83294	0.123156	0.00123	1.40E-08	9.49E-07	0.989005	0.009764
106	-1.83294	0.123156	0.00123	1.17E-08	5.91E-07	0.989005	0.009764
107	-1.83294	0.123156	0.00123	5.68E-09	3.87E-07	0.989005	0.009764
108	-1.83294	0.123156	0.00123	3.82E-09	2.62E-07	0.989005	0.009764
109	-1.83294	0.123156	0.00123	2.62E-09	1.81E-07	0.989005	0.009764
110	-1.83294	0.123156	0.00123	1.93E-09	1.34E-07	0.989005	0.009764
111	-1.83294	0.123156	0.00123	1.42E-09	1.01E-07	0.989005	0.009764

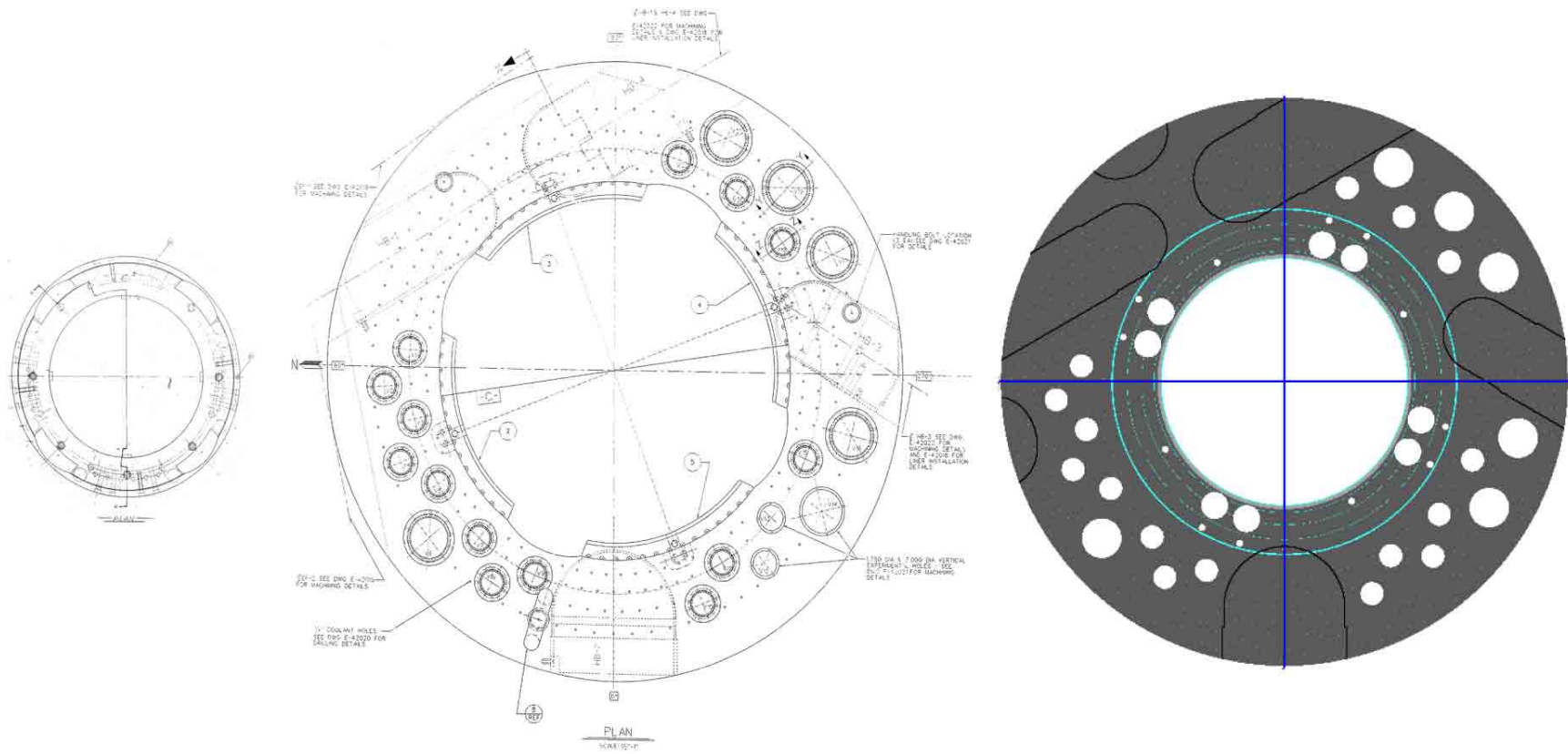


Fig. 5. The beryllium reflector. Shown on the left and center from HFIR drawing E-42415 and E-42017, and on the right from the MCNP model. The MCNP reflector model includes cut-outs for the vertical experiments and beam tubes, all of which are also included in the model. (Key: gray—beryllium, blue—water.)

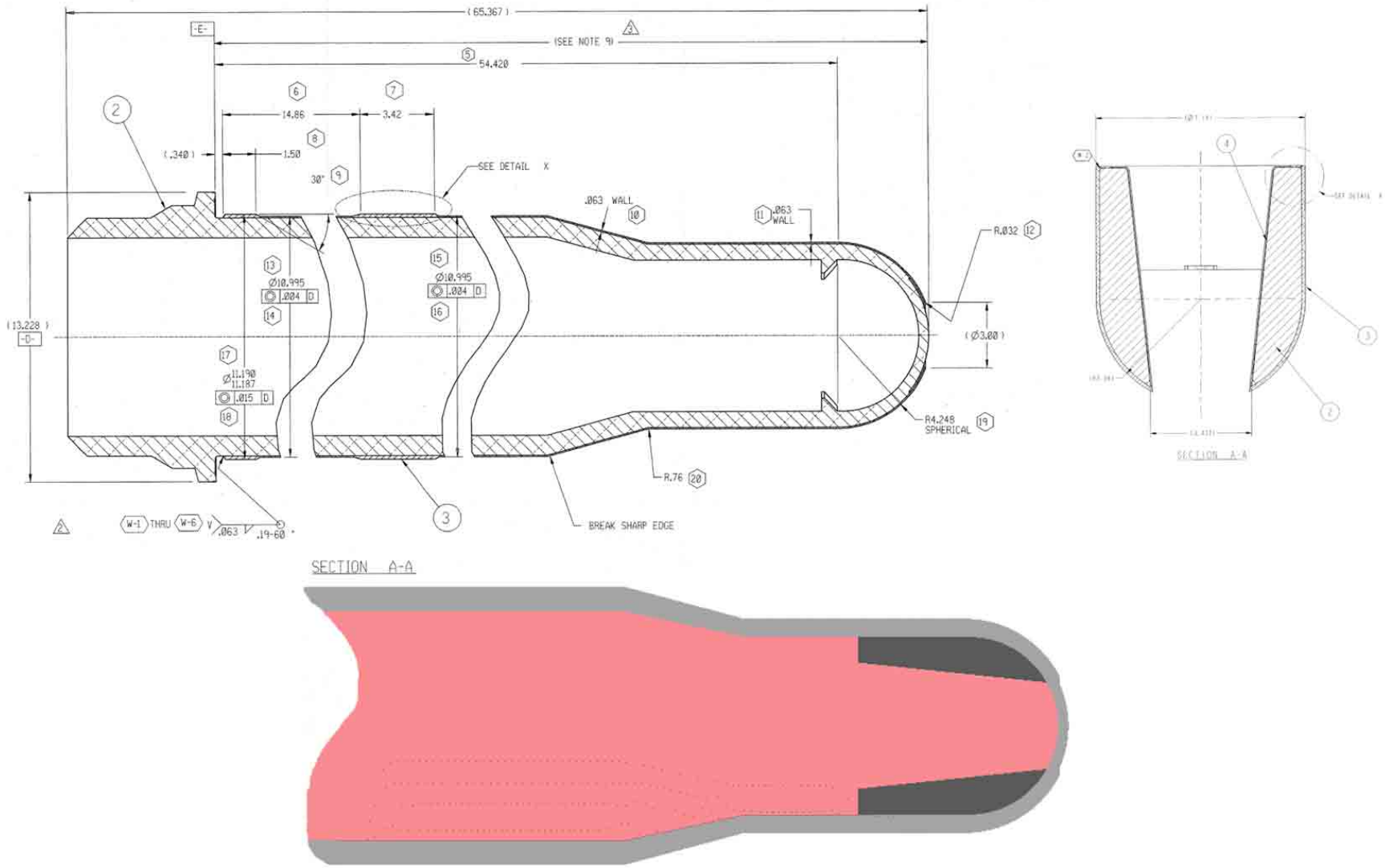


Fig. 6. Horizontal beam tube 2. Shown above from HFIR drawings M-11537-OH-061 and M-11537-OH-084 and below from the MCNP model. (Key: dark gray—beryllium, gray—aluminum, pink—helium.)

container, surrounded by water coolant, inside an aluminum shell that is placed in the reflector. The tube changes diameter as it leaves the reflector area. In the smaller diameter portion of the beam tube, there are beryllium inserts, modeled as seven layers of beryllium with different levels of lithium and helium.

Beam tube 3, shown in Fig. 7, is similar to the first beam tube. All of the horizontal beam tubes are axially located at the reactor midplane.

2.6 HORIZONTAL BEAM TUBE 4 AND COLD SOURCE

The model for the fourth horizontal beam tube is an aluminum tube, which changes diameter after leaving the reflector area. Inside the tube is a model of the cold source moderator—an aluminum housing filled with hydrogen. The two tubes of hydrogen extend outward with the beam tube through the reactor vessel. This beam tube is shown in Fig. 8. In the pool, between the reactor vessel and the biological shield, the model of the beam tube again increases in diameter. The hydrogen in the cold source and beam tube would be at a nominal temperature of 20 K and a density of 0.0726 g/cm³ [0.043381 atoms/(b cm)] when the cold source is operating. In the hf2004 model, the nuclear thermal scattering dataset assigned to hydrogen in this region is the MCNP 20 K hpara.01t dataset. No TMP or TMTME cards have been added to the H₂ regions. See Sect. 2.9 for notes about special cross section sets.

2.7 REACTOR VESSEL AND CONCRETE SHIELDING

The rest of the MCNP model describes the coolant, the pool, the reactor vessel and the concrete biological shield. The reactor vessel components and densities are listed in Table 17, and the geometry is shown in Fig. 9. The reactor vessel model consists mostly of carbon steel with a thin stainless steel liner on both the inside and outside surfaces. The vessel and concrete shield are modeled as cylindrical regions extending 150 cm above and below the reactor midplane. Volumes above and below these levels were not modeled because most of the neutron events of interest (the fuel and beam tubes) are occurring at the reactor midplane.

2.8 DETAILED BEAM TUBE GEOMETRIES

Detailed geometries for each beam tube are supplied in the auxiliary file, hf2004.aux. These geometries subdivide the aluminum containers into smaller regions so that detailed heating studies could be performed. Users can swap any of the detailed beam models for the simple models that are included in the standard model, hf2004.

2.9 SPECIAL CROSS SECTIONS USED IN HF245

HF245 used special cross section libraries that are not part of the standard release of MCNP. For liquid hydrogen, S(α,β) data were obtained from R. E. Williams (National Institute for Standards and Technology) for both the para- and ortho-hydrogen states. The ZAID numbers for these states are 1014 and 1016, so that they can be mixed together. MCNP will not mix two thermal scattering datasets for the same ZAID. For example, a material consisting of 25% para-H₂ and 75% ortho-H₂ would have a material listing of

```
m100 1001.50c -0.25 1001.50c -0.75
mt100 hpara.01t hortho.01t
```

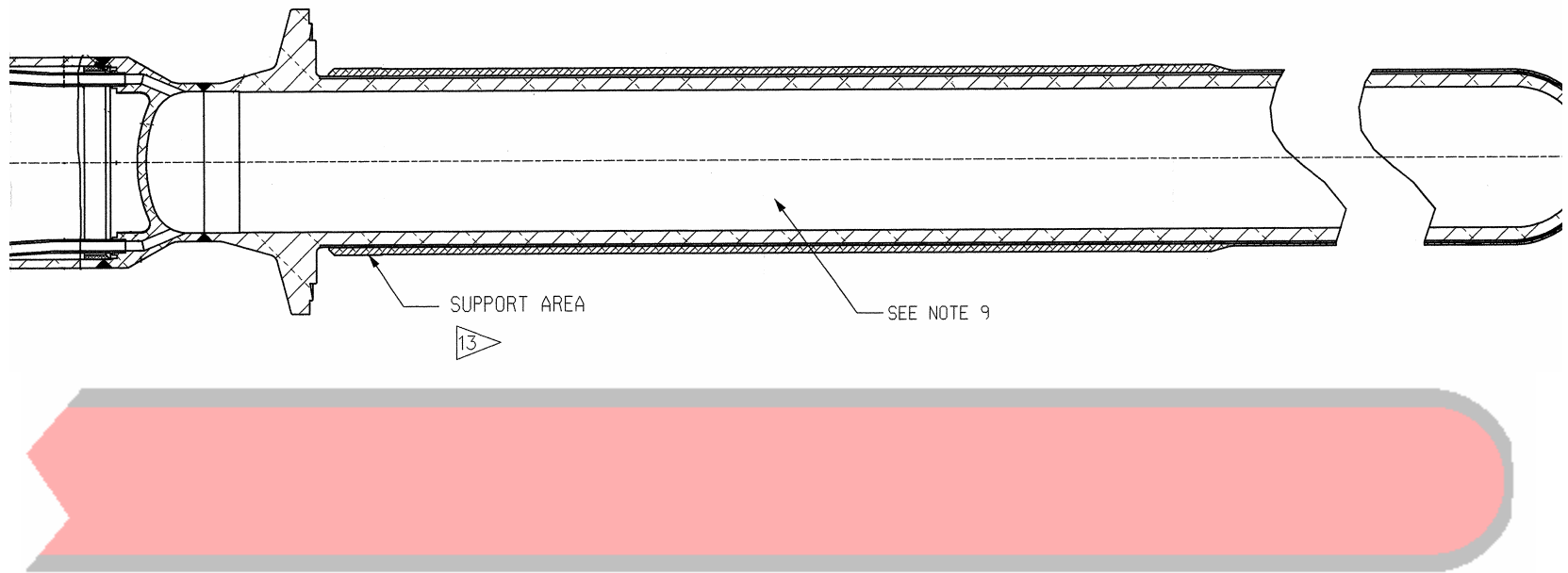


Fig. 7. Horizontal beam tube 3. Shown above from HFIR drawing M-11537-OH-039 and below from the MCNP model. (Key: gray—aluminum, pink—helium.)

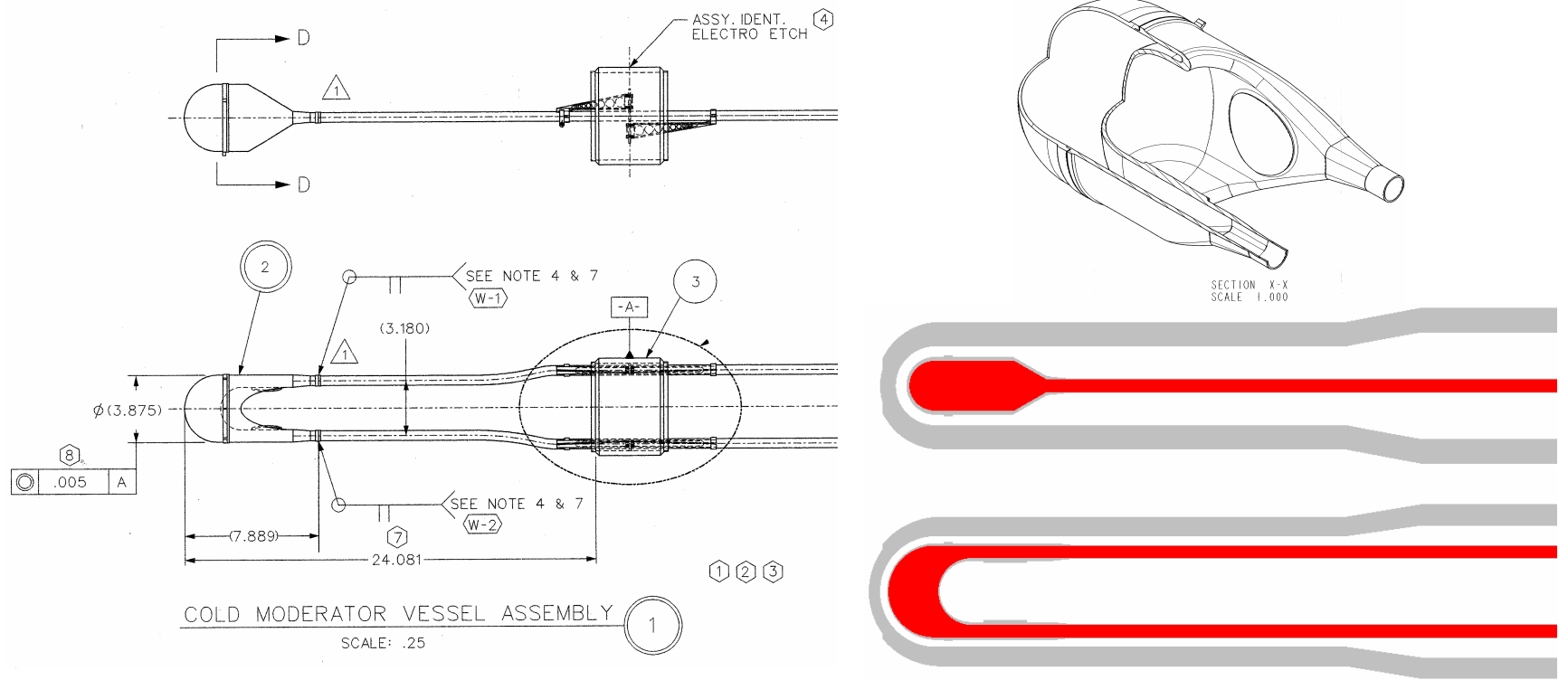


Fig. 8. The cold source moderator inside horizontal beam tube 4. Shown on the left and upper right from HFIR drawings M-11530-CS-313 and M-11530-CS-034 and on the lower right from the MCNP model. (Key: gray—aluminum, red—hydrogen.)

Table 17. Isotopic weight fractions and densities for pool, vessel and biological shield materials

Material code			1	40	50	62
			Water	Stainless steel 304	Carbon steel	Barytes concrete
Density, g/cm ³			-1	-8	-8.16	-3.09725
/(b cm)			0.10031	0.08711	0.09121	0.07760
1001	50c	H	0.1119			9.035E-03
5010	50c	B				1.804E-03
5011	56c	B				8.032E-03
6012	50c	C			0.01	
8016	50c	O	0.8881			3.578E-01
11023	50c	Na				3.915E-03
12000	50c	Mg				2.008E-03
13027	50c	Al				1.084E-02
14000	50c	Si				1.887E-02
16032	50c	S				9.209E-02
20000	50c	Ca				6.996E-02
22000	50c	Ti				3.411E-03
24000	50c	Cr		0.19		
25055	50c	Mn		0.02		5.019E-03
26000	55c	Fe		0.695	0.99	2.048E-02
28000	50c	Ni		0.095		
56138	50c	Ba				3.967E-01

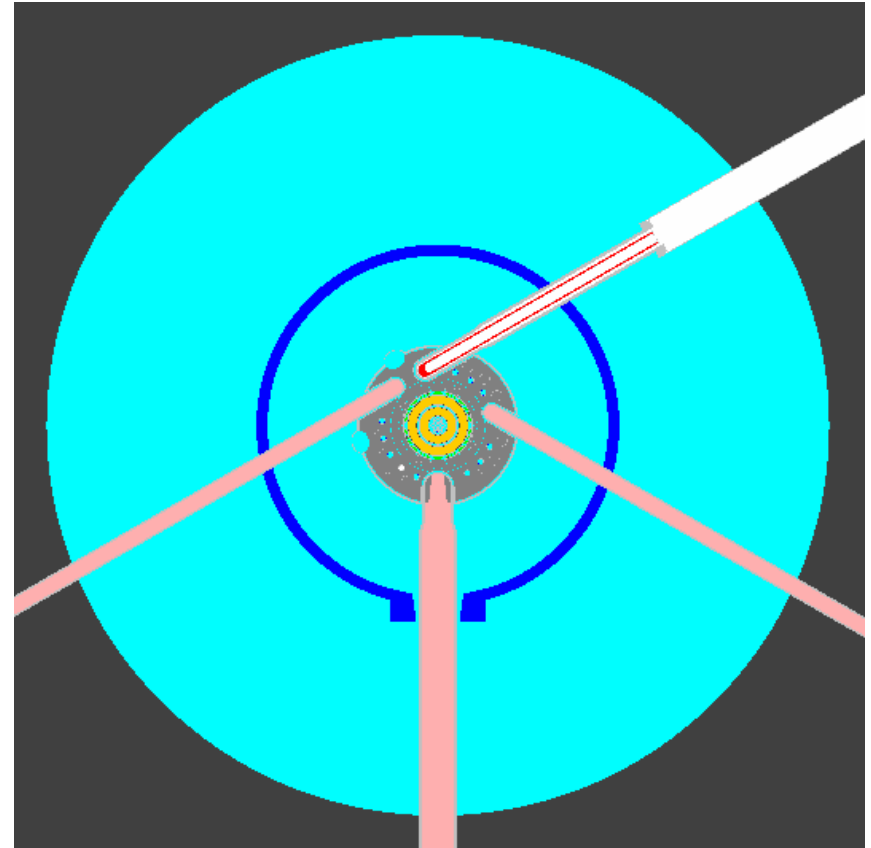
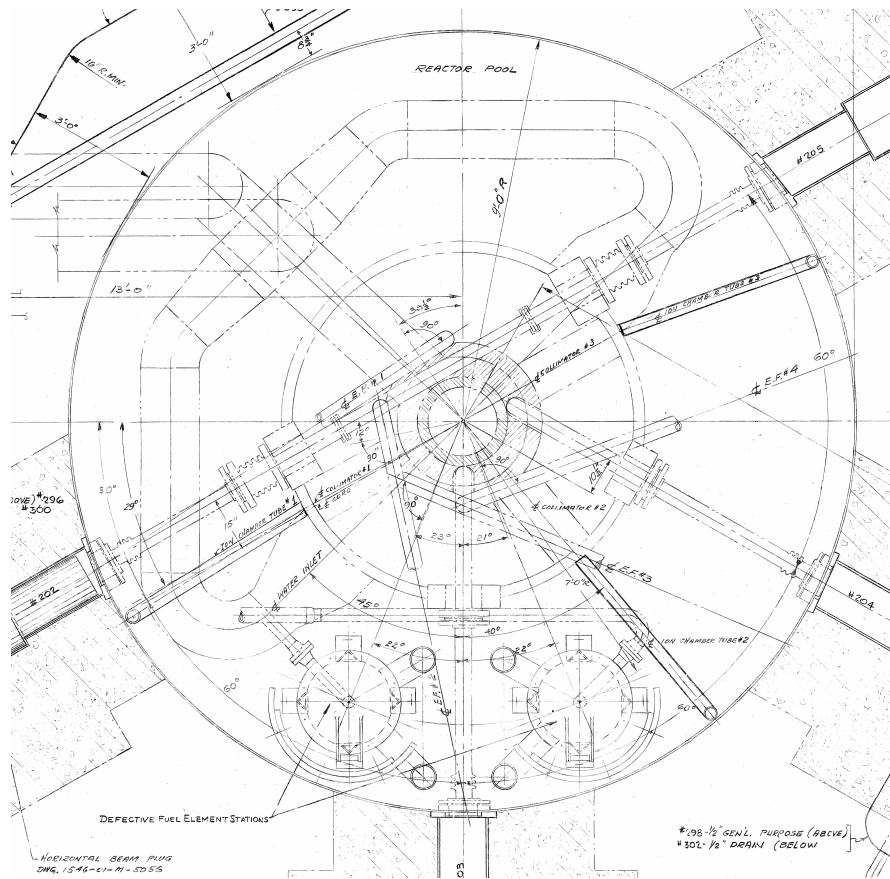


Fig. 9. The pool region. Shown on the left from HFIR drawing 1546-01-M-5022 and on the right from the MCNP model. (Key: yellow—fuel; green—control elements; light blue—water; dark blue—steel; gray—aluminum; dark gray—concrete.)

and will generate a warning, and then only use the ortho thermal dataset. A listing of

```
m100 1014.51c -0.25 1016.51c -0.75  
mt100 parah.96t orthoh.96t
```

should correctly model the mixed-state hydrogen. Presumably, these libraries were also more accurate than the standard MCNP $S(\alpha,\beta)$ libraries for hydrogen at the time (~1995). These libraries do seem to be about the same as the standard hydrogen libraries that are a part of MCNP4C (Breismeister 2000).

One of the uses of HF245 was to calculate the nuclear heating of the cold source components. Some aspects of this are not taken into account in a single run of MCNP but can be with specially made cross sections. First, in aluminum, when a neutron is absorbed by ^{27}Al , ^{28}Al is formed. This isotope has a half-life of only 2.24 min and decays by emitting a beta particle with a maximum energy of 2.863 MeV (average energy of 1.247 MeV). The resulting excited ^{28}Si nucleus then gives off a 1.779-MeV gamma ray as it relaxes to the ground state. To include the beta heating in calculations, one has to determine the $^{27}\text{Al}(n,\gamma)^{28}\text{Al}$ reaction rate (equivalent to the equilibrium activity) for every cell containing aluminum, compute the dose from that activity, and then add that to the MCNP calculated heating. Further, those $^{27}\text{Al}(n,\gamma)^{28}\text{Al}$ reaction rates would have to be used to construct a new gamma source, which would be run in another MCNP calculation and added to the original MCNP neutron transport calculation and ^{28}Al beta decay doses. HF245 instead uses special aluminum-27 cross section data that includes the ^{28}Si 1.779-MeV gamma in the $^{27}\text{Al}(n,\gamma)^{28}\text{Al}$ reaction, thereby producing the correct result in a single MCNP run. The decay gammas are included in the transport so all that needs to be added to the MCNP heating tallies is the beta heating.

For uranium fission, MCNP includes the prompt gamma rays but not the gamma rays from the fission products (delayed gamma rays). Normally, to include these gamma rays in the heating calculation, the source distribution from the first MCNP neutron transport calculation would be used to construct a gamma source distribution with an appropriate energy spectrum representing the delayed gammas. The gammas would then be transported in a separate calculation, and the heating values would be added to the original neutron transport heating values. Instead, HF245 used a ^{235}U cross section that included fission product gamma rays with the normal prompt gamma rays, obtaining both the neutron and gamma transport in one calculation.

These extra files are included on the CD that accompanies this report and may be used in the new hf2004 model if desired. Follow the directions given in HF245/notes.txt for adding these libraries.

3. COMPARISONS TO MEASURED VALUES

MCNP tallies are typically normalized to one source particle. To obtain absolute flux values or reaction rates, the tally answers must be multiplied by the true source strength. For a reactor such as HFIR in which power comes from mostly one isotope, ^{235}U , the source strength, S , can be found by a simple relation to the reactor power:

$$S = (2.43 \text{ neutrons/fission}) * (85 \times 10^6 \text{ W}) / [(200.7 \text{ MeV/fission})(1.602177 \times 10^{-13} \text{ J/MeV})] \\ = 6.4234 \times 10^{18} \text{ neutrons/s}$$

The following comparisons used this (or a similar) relation to modify MCNP tallies. Calculations were performed with the Research Reactors Division configuration-controlled version of MCNP 5—the MCNP5_RSICC 1.20 release (X-5 Monte Carlo Team 2003)—and were performed on a LINUX cluster (designated cpile.ornl.gov).

3.1 TARGET REGION PEAK THERMAL NEUTRON FLUX

Cheverton and Sims (1966), in their intralaboratory correspondence titled “Determination of the Target Region Thermal Neutron Flux from the Results of Recent Cobalt Activation Experiments in the HFIR,” described a $^{59}\text{Co}(n,\gamma)^{60}\text{Co}$ experiment to measure the thermal flux at the center of the HFIR. Their letter states:

Our analysis of the recent experimental data indicates that the actual thermal flux in the flux trap is essentially the same as that predicted; however, the accuracy associated with the experimental value is probably no better than about ± 10 to $\pm 15\%$. The flux values reported herein correspond to the thermal neutron spectrum that existed in the experiment at the location of the irradiated flux monitor wire. This location was on the longitudinal core axis at the horizontal midplane.

They irradiated a 10.386-mg wire, 0.0954% ^{59}Co by weight, for 10 h at 89 MW. After 199 h of decay, they measured the ^{60}Co activity. From that, they calculated the saturation activity per target atom per unit reactor power to be 1.14×10^{-9} dps/MW/atom. Finally, using cross sections from various computer codes, they calculated the thermal flux per unit reactor power to be 3.5×10^{13} neutrons/($\text{cm}^2 \cdot \text{s} \cdot \text{MW}$).

The hf2004 model was used to calculate both the thermal neutron flux and the ^{60}Co production rate per target atom (which is equivalent to the saturation activity). The thermal flux was taken as the average over 1 cm^3 of the center rod in the target, from 0 to 0.414 eV. The ^{60}Co production rate was calculated using the total flux of the same volume but multiplied by the $^{59}\text{Co}(n,\gamma)$ cross section. Note that thermal flux in the center region is greatly influenced by the other materials in the target. The current MCNP HFIR model most likely does not model the target used in 1966. Results are shown in Table 18.

3.2 HYDRAULIC TUBE NEUTRON FLUXES

Mahmood et al., 1995 measured the neutron flux in the hydraulic tube (position B3 in the central target region) using a variety of activation wires, a fission monitor, and helium accumulation flux monitors (HAFMs). Measurements were taken in five of the nine axial positions

Table 18. Measured and calculated thermal fluxes and saturation activities in the center of the HFIR reactor

Study	Thermal flux [/(cm ² s)/MW]		Saturation activity (dps/MW)	
Cheverton and Sims	3.50E+13	10.0%	1.14E-09	10.0%
MCNP—BOC	2.61E+13	0.9%	8.87E-10	1.2%
C/E	0.75		0.78	
MCNP—EOC	2.50E+13	0.9%	8.50E-10	1.4%
C/E	0.71		0.75	

(HT-1, HT-3, HT-5 HT-7 and HT-9). Flux measurements included total flux, thermal flux, fast flux greater than 0.1 MeV and fast flux greater than 1.0 MeV. The experiments included the following:

	HT-1	HT-3	HT-5	HT-7	HT-9
Activation wires					
²⁷ Al(n,α) ²⁴ Na	1	1	1	1	1
⁴⁶ Ti(n,p) ⁴⁶ Sc	1	1	1	1	1
⁵⁴ Fe(n,p) ⁵⁴ Mn	1	1	1	1	1
⁵⁸ Ni(n,p) ⁵⁸ Co	1	1	1	1	1
⁶³ Cu(n,α) ⁶⁰ Co	1	1	1	1	1
⁵⁹ Co(n,γ) ⁶⁰ Co	1	1	1	1	1
¹⁰⁹ Ag(n,γ) ^{110m} Ag	1	1	1	1	1
¹⁹⁷ Au(n,γ) ¹⁹⁸ Au	1	1	1	1	1
Thermal activation (bare/Cd)					
⁵⁹ Co(n,γ) ⁶⁰ Co	1 set		1 set		
¹⁰⁹ Ag(n,γ) ^{110m} Ag	1 set		1 set		
¹⁹⁷ Au(n,γ) ¹⁹⁸ Au	1 set		1 set		
Fission monitor					
²³⁷ Np(n,f) ¹⁴⁰ Ba	1		1		
HAFMs					
⁶ Li(n,He)	1	1	1	1	1
⁹ Be(n,He)	1	1	1		
¹⁰ B(n,He)	1	1	1	1	1

The hf2004 model was used to calculate the same fluxes, both at BOC and EOC. Flux tallies (F4) were made over the entire capsule position, binned by energy. The thermal cutoff energy was 0.414 eV. The results of the MCNP calculations are shown in Figs. 10–14 along with the flux values obtained from each type of experimental monitor. MCNP one-sigma uncertainties averaged 1.1%, with all $\leq 2.6\%$, which are smaller than the symbols used in the figures.

In each of the figures, the experimental measurements for a given axial position are broken into four groups, depending on what type of monitor they are. As well as being colored differently, these four groups are shifted horizontally away from the axial position number (1, 3, 5, 7, or 9), so that they can be more easily differentiated.

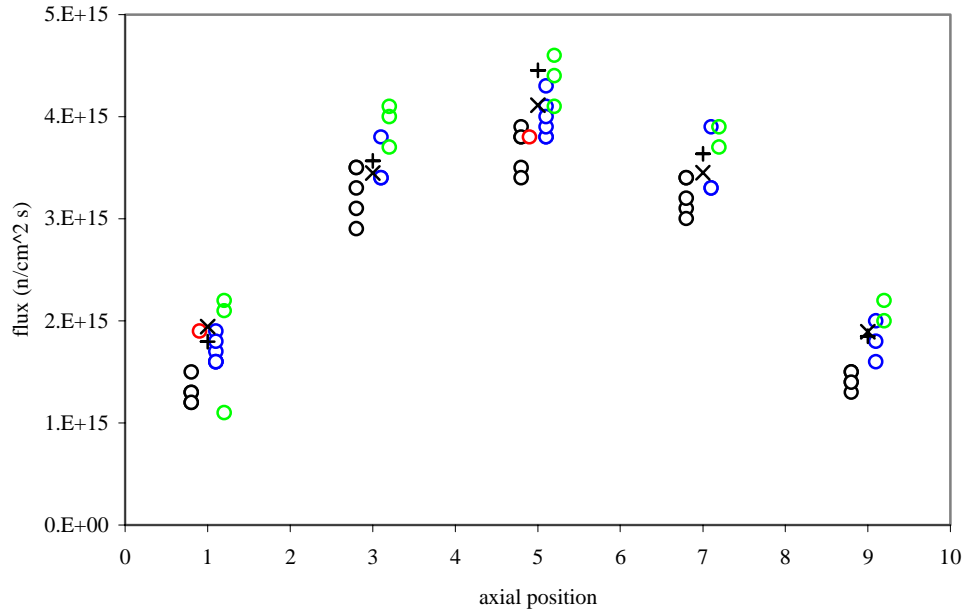


Fig. 10. Total fluxes—ORNL/TM-12831 and the hf2004 model. Symbol key: open circles—experimental flux measurements; plus signs—BOC calculations; “x” symbols—EOC calculations. Color key for experimental values: black—activation wires; blue—thermal activation wires; red—fission monitor; green—HAFM.

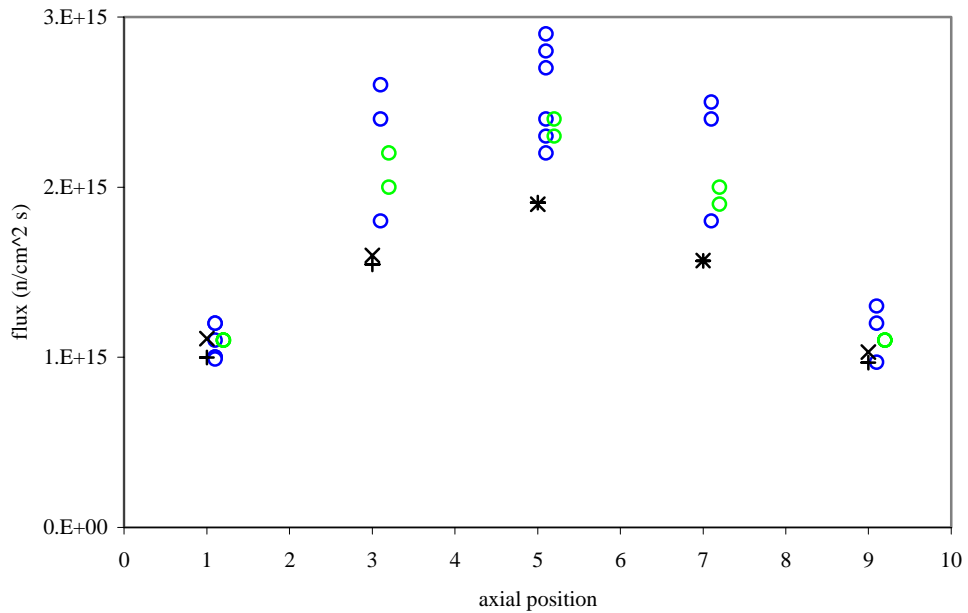


Fig. 11. Thermal fluxes—ORNL/TM-12831 and the hf2004 model. Symbol key: open circles—experimental flux measurements; plus signs—BOC calculations; “x” symbols—EOC calculations. Color key for experimental values: blue—thermal activation wires; green—HAFM.

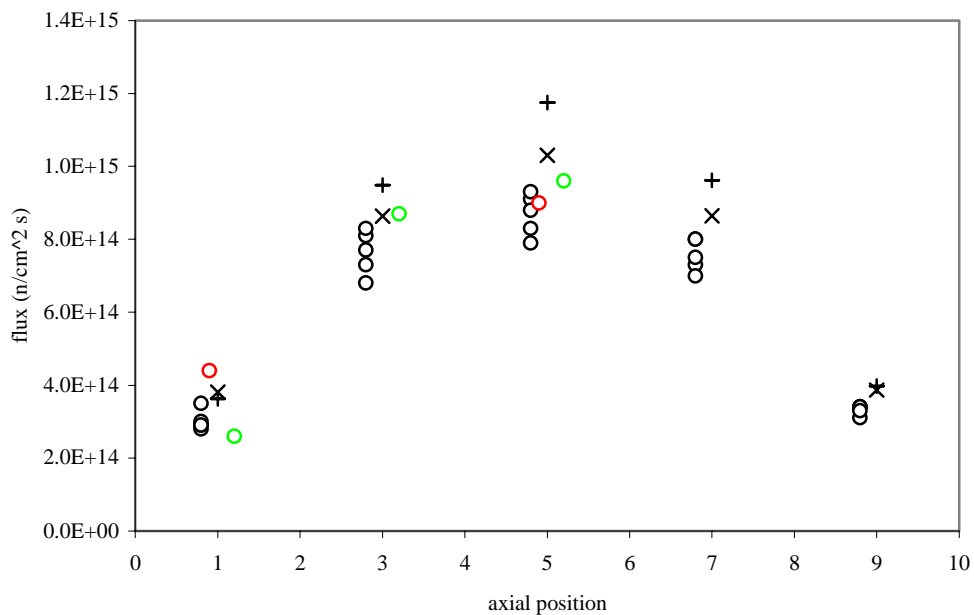


Fig. 12. Fast fluxes (>0.1 MeV)—ORNL/TM-12831 and the hf2004 model. Symbol key: open circles—experimental flux measurements; plus signs—BOC calculations; “x” symbols—EOC calculations. Color key for experimental values: black—activation wires; red—fission monitor; green—HAFM.

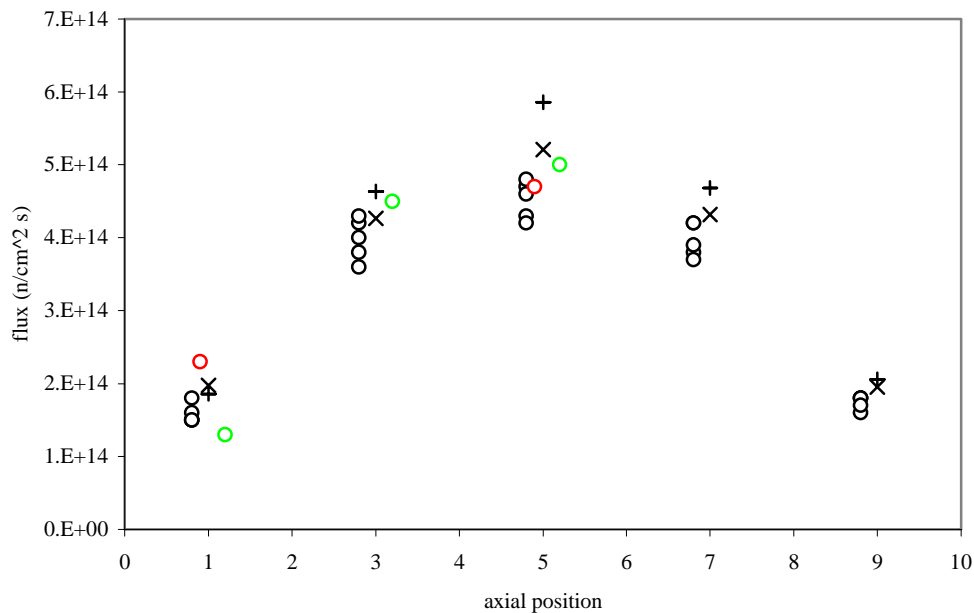


Fig. 13. Fast fluxes (>1.0 MeV)—ORNL/TM-12831 and the hf2004 model. Symbol key: open circles—experimental flux measurements; plus signs—BOC calculations; “x” symbols—EOC calculations. Color key for experimental values: black—activation wires; red—fission monitor; green—HAFM.

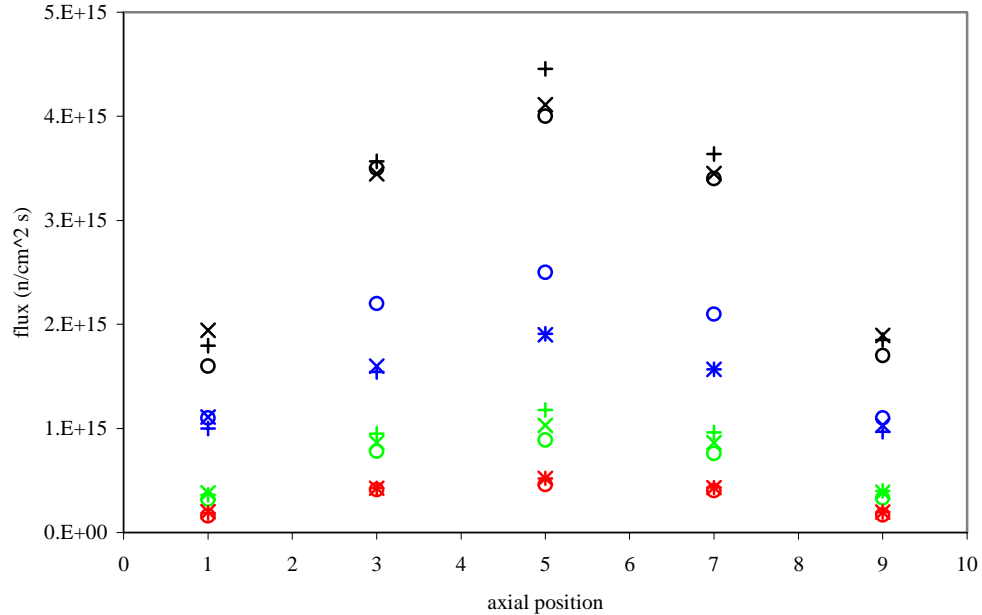


Fig. 14. Average fluxes—ORNL/TM-12831 (Table 14) and the hf2004 model. Symbol key: open circles—experimental flux averages; plus signs—BOC calculations; “x” symbols—EOC calculations. Color key: black—total flux; blue—thermal flux; green—fast flux (>0.1 MeV); red—fast flux (>1.0 MeV).

It appears that the total flux values match very well. MCNP thermal flux values are consistently low, which may be due to differences between the model and experiment as to what other materials are present in the target region. Calculated to experimental measurement ratios are listed in Table 19.

Table 19. Ratios of the MCNP calculated flux values to the measured flux values in the hydraulic tube for both BOC and EOC

Flux	HT-1		HT-3		HT-5		HT-7		HT-9	
	BOC	EOC								
Total	1.12	1.21	1.02	0.99	1.11	1.03	1.07	1.02	1.09	1.11
Thermal	0.91	1.01	0.70	0.73	0.76	0.76	0.75	0.75	0.88	0.94
Fast (>0.1 MeV)	1.13	1.19	1.22	1.11	1.32	1.16	1.27	1.14	1.20	1.17
Fast (>1.0 MeV)	1.16	1.24	1.13	1.04	1.27	1.13	1.17	1.08	1.21	1.15

3.3 REFLECTOR THERMAL NEUTRON FLUXES

Thermal flux measurements have been made in two of the experimental facilities located in or on the edge of the beryllium reflector by Glasgow (Glasgow 2004a). The small vertical experimental facility (VXF-7) tube is located 39.37 cm from the center of the reactor, inside the beryllium reflector. The engineering facility (EF-2) is located 55.88 cm from the reactor center, at the outer edge of the beryllium reflector. Measurements were made with two monitors, dilute gold

(0.1%) and manganese (0.087%). Flux values were developed from the set of simultaneous activation equations.

Calculations for thermal (energy < 0.414 eV) and epithermal fluxes (0.414 eV to 6 eV) were made for small volumes in the experimental facilities where they cross the reactor midplane. A comparison of the calculated values and the measured values is presented in Table 20. Glasgow indicated that his epithermal values may contain contributions from fast neutrons, which should be small.

The calculated values for the VXF-7 tube are 30 to 70% higher than the measurements by Glasgow. In EF-2, the MCNP calculated values are 70 to 100% higher than the measurements. This may be due to inadequate modeling, as suggested by Glasgow (Glasgow 2004b):

The fluence rate has always been overestimated for the flight tubes. Calculations even from the 1980's are not much different than those (in this work). The PT-2 fluence rate, for example, is predicted to be about $1E+14$ for EF-3 and was measured to be $5E+13$. This is so common that I think there is a systematic problem with the calculations. The measured numbers have been verified by multiple nuclear reactions, analysts, equipment and investigators. They are obtained in the polyethylene rabbits without the polyethylene insert. Irradiation duration is typically 20 seconds for PT-1 and 30-60 seconds for PT-2. Time uncertainty is less than 1 second for either case. Since I have seen it before (I can show you flux estimates for PT-2 prior to its installation in 1986) I am not surprised by your findings of about 2X overestimation. Our total flux uncertainty is about 5% but is not rigorously propagated. I have often speculated about the poor measurement-calculation agreement but I have no fruits to offer.

and Farrar (Farrar 2004):

I have not ever seen the computer models or results, but I've always wondered how rigorously the P-tube was modeled. There's an Al liner, a significant water gap, a stainless steel flight tube surrounded by a host of stainless steel service tubes, and then the sample is enclosed in a polyethylene rabbit. The ... neutrons have a number of (absorbers) to get through to get to the foil.

The hf2004/HF245 models for the pneumatic tube (VXF-7) contain the aluminum liner and an aluminum flight tube, but the remainder of the region is modeled as air. Other small vertical experiments in the beryllium reflector are modeled with stainless steel flight tubes. This area of the model could probably be improved to better match the experiments.*

3.4 MULTIPLICATION FACTOR

The fuel region of the MCNP model was written by Gehin 1996. At that time, the k_{eff} was calculated for both the BOC and the EOC models. Those values and values calculated by the current hf2004 model are shown in Table 21.

* For example, preliminary studies show that by changing the large aluminum liner to a smaller diameter steel liner, adding four steel service tubes, and adding a polyethylene rabbit capsule, the MCNP calculated BOC thermal flux drops 20%, getting much closer to the experimentally measured values. Even closer agreement might be obtained by having MCNP calculate the activation of the foils and comparing that to the experimental measurements.

Table 20. Values calculated with the MCNP model and Glasgow 2004

Quantity	Calculated—BOC		Calculated—EOC		David Glasgow		
	Value	Relative error	Value	Relative error	5/14/04	5/19/04	5/20/04
VXF-7	Thermal flux (/cm ² s)	5.74E+14	0.8%	7.22E+14	0.7%		
	Epithermal flux (/cm ² s)	4.20E+13	3.0%	4.49E+13	2.9%		
	Thermal/epithermal ratio	13.7	3.1%	16.1	3.0%		
EF-2	Thermal flux (/cm ² s)	7.12E+13	1.4%	8.74E+13	1.3%	4.32E+13	
	Epithermal flux (/cm ² s)	8.99E+11	5.1%	1.12E+12	4.6%		
	Thermal/epithermal ratio	79.2	5.3%	78.0	4.8%	353	

Table 21. Values and one-sigma relative uncertainties for k_{eff} calculated with MCNP models

	BOC		EOC	
	Value	Relative error	Value	Relative error
Gehin, 1996	1.0085	0.0010	1.0070	0.0006
hf2004	1.0073	0.0002	1.0056	0.0002

4. SUMMARY

The HFIR model hf2004 and its auxiliary portions in hf2004.aux are a simple, clean model of the HFIR. A model for a particular point in the fuel cycle, with the appropriate fuel materials and vertical settings for the control elements can easily be built using these files. Various validation studies show that the model predicts total flux in the core region well and fluxes in the reflector experiments to a fair degree. Future work should center on making the model reflect the materials and geometry of the current HFIR.

REFERENCES

- Binford, F. T. and E. N. Cramer, 1968. *The High Flux Isotope Reactor, A Functional Description*, ORNL-3572 (Rev. 2), Oak Ridge National Laboratory, Oak Ridge, Tennessee.
- Breismeister, J. F., ed., 2000. *MCNP Version 4c, Monte Carlo N-Particle Transport Code System*. LA-13709-M, Los Alamos National Laboratory, Los Alamos, New Mexico.
- Bucholz, J. A., 2000. *Source Terms for HFIR Beam Tube Shielding Analyses, and a Complete Shielding Analysis of the HB-3 Tube*. ORNL/TM-13720, Oak Ridge National Laboratory, Oak Ridge, Tennessee.
- Cheverton, R. D. and T. M. Sims, 1966. *Determination of the Target Region Thermal Neutron Flux from the Results of Recent Cobalt Activation Experiments in the HFIR*. Intra-laboratory correspondence dated September 8, 1966, Oak Ridge National Laboratory, Oak Ridge, Tennessee.
- Cheverton, R. D. and T. M. Sims, 1971. *HFIR Core Nuclear Design*. ORNL-4621, Oak Ridge National Laboratory, Oak Ridge, Tennessee.
- Farrar, M. B. 2004. Oak Ridge National Laboratory. Personal communication to R. T. Primm III, Oak Ridge National Laboratory, October 4.
- Gehin, J. C., 1996. *Model Development and Benchmarking* presentation at the HFIR Cold Source Review, March 11.
- Glasgow, D. C. 2004a. Oak Ridge National Laboratory. Personal communication to R. T. Primm III, Oak Ridge National Laboratory, June 2.
- Glasgow, D. C. 2004b. Oak Ridge National Laboratory. Personal communication to R. T. Primm III, Oak Ridge National Laboratory, October 1.
- Johnson, J. O. 2004. *Applicability of the Monte Carlo N-Particle (MCNP) Transport Code System to the Assessment of Nuclear Heating*, ORNL-2004-178, Oak Ridge National Laboratory, Oak Ridge, Tennessee.
- Mahmood, S. T., S. Mirzadeh, K. Farrell, J. V. Pace III, and B. M. Oliver, 1995. *Neutron Dosimetry of the HFIR Hydraulic Facility*. ORNL/TM-12831, Oak Ridge National Laboratory, Oak Ridge, Tennessee.
- Sease, J. D., 1998. *Fabrication of Control Rods for the High Flux Isotope Reactor*, ORNL/TM-9365/R1, Oak Ridge National Laboratory, Oak Ridge, Tennessee.
- Sulfredge, C. D., R. L. Sanders, D. E. Peplow and R. H. Morris, 2002. "Graphical Expert System for Analyzing Nuclear Facility Vulnerability," *Transactions of IITSEC: Interservice/Industry Training, Simulation and Education Conference, The Power of Simulation: Transforming Our World*, December 2002, Orlando, Florida.
- X-5 Monte Carlo Team, 2003. *MCNP—A General Monte Carlo N-Particle Transport Code, Version 5. Volume I: Overview and Theory*, LA-UR-03-1987, Los Alamos National Laboratory, Los Alamos, New Mexico.

Appendix A
FILES ON THE ACCOMPANYING CD

Appendix A

FILES ON THE ACCOMPANYING CD

Attached to this report is a CD containing the hf2004 model, auxiliary file, original Bucholz model, MCNP input deck used for the comparisons and some of the materials listed in the reference.

Filename	Description
hf2004	The simplified HFIR MCNP model (geometry and materials)
hf2004.aux	Auxiliary material for hf2004—BOC/EOC, more detailed beam tubes, etc.
ornl_tm_2004_237.pdf	Electronic version of this ORNL TM
HF245/ HF245	The original Bucholz model, before any simplifications
hh2bike1	Data for liquid hydrogen $S(\alpha,\beta)$
rmcfig1	Al-27 with Al-28 beta decay and gamma rays
u235frg1	U-235 with fission product delayed gammas
xmdir.extras	Extra lines to add to the system xmdir file
reference/ cf-70-7-51.pdf	Haack, L. A., 1970. <i>Gamma Heating Rates in HFIR Experimental and Production Facilities—Method of Extracting Values from Existing Data</i> . Letter to HFIR File, Oak Ridge National Laboratory, Oak Ridge, TN, July, 30. (For Internal Use Only.)
cole10_19_66.pdf	Unknown, 1966. <i>Fast Threshold Activation Measurements of an HFIR Core Configuration with Plutonium Targets Inserted</i> . A letter/calculation report to T. E. Cole, R. V. McCord, and C. Cagle, October (?), 1966.
distribution10_8_66.pdf	Cheverton, R. D. and T. M. Sims, 1966. <i>Determination of the Target Region Thermal Neutron Flux from the Results of Recent Cobalt Activation Experiments in the HFIR</i> . Intra-laboratory correspondence dated September 8, 1966, Oak Ridge National Laboratory, Oak Ridge, TN.
farrar.txt	Farrar, M. B. 2004. Oak Ridge National Laboratory. Personal communication to R. T. Primm III, Oak Ridge National Laboratory, October 4.
glasgow.txt	Glasgow, D. C. 2004. Oak Ridge National Laboratory. Personal communication to R. T. Primm III, Oak Ridge National Laboratory, June 2.
glasgow2.txt	Glasgow, D. C. 2004. Oak Ridge National Laboratory. Personal communication to R. T. Primm III, Oak Ridge National Laboratory, October 1.
hfirmodl.ppt	Gehin, Jess, 1996. <i>Model Development and Benchmarking</i> presentation at the HFIR Cold Source Review, March 11.
ornl_tm2004_178.pdf	Johnson, J. O. 2004. <i>Applicability of the Monte Carlo N-Particle (MCNP) Transport Code System to the Assessment of Nuclear Heating</i> , ORNL-2004-178, Oak Ridge National Laboratory, Oak Ridge, TN.

ornl_tm_9365_r1.pdf	Sease, J. D., 1998. <i>Fabrication of Control Rods for the High Flux Isotope Reactor</i> , ORNL/TM-9365/R1, Oak Ridge National Laboratory, Oak Ridge, TN.
ornl_tm_12831.pdf	Mahmood, S. T., S. Mirzadeh, K. Farrell, J. V. Pace III, B. M. Oliver, 1995. <i>Neutron Dosimetry of the HFIR Hydraulic Facility</i> . ORNL/TM-12831, Oak Ridge National Laboratory, Oak Ridge, TN.
ornl_tm_12831.xls	Selected tables from ORNL/TM-12831, in a usable spreadsheet.
ornl_tm_13720.pdf	Bucholz, J. A., 2000. <i>Source Terms for HFIR Beam Tube Shielding Analyses, and a Complete Shielding Analysis of the HB-3 Tube</i> . ORNL/TM-13720, Oak Ridge National Laboratory, Oak Ridge, TN.
sulfredge2002.pdf	Sulfredge, C. D., R. L. Sanders, D. E. Peplow and R. H. Morris, 2002. "Graphical Expert System for Analyzing Nuclear Facility Vulnerability," <i>Transactions of IITSEC: Interservice/Industry Training, Simulation and Education Conference, The Power of Simulation: Transforming Our World</i> , December 2002, Orlando, Florida.
drawings/ *.tif	HFIR drawings downloaded from the HFIR drawing database
other/ *.pdf	Other HFIR related papers
comparisons/ benXb benXe benXb benXe benchX.xls benXb.o benXe.o	(For comparisons listed in Sect. 3, where X is 1, 2, 3, or 4) MCNP input for BOC version of hf2004 for comparison X MCNP input for EOC version of hf2004 for comparison X Batch file to run benXb Batch file to run benXe Results of MCNP runs, data reduction and the final tables in this report MCNP output for BOC version of hf2004 for comparison X MCNP output for EOC version of hf2004 for comparison X

INTERNAL DISTRIBUTION

- | | |
|--------------------|---------------------------------|
| 1. C. W. Alexander | 14. D. J. Newland |
| 2. F. A. Alpan | 25. C. V. Parks |
| 3. L. W. Boyd | 16–20. D. E. Peplow |
| 4. E. D. Blakeman | 21–25. R. T. Primm III |
| 5. J. A. Bucholz | 26. I. Remec |
| 6. D. H. Cook | 27. J. P. Renier |
| 7. M. B. Farrar | 28. D. L. Selby |
| 8. J. D. Freels | 29. C. O. Slater |
| 9. F. X. Gallmeier | 30. K. A. Smith |
| 10. J. C. Gehin | 31. C. C. Southmayd |
| 11. R. W. Hobbs | 32. H. R. Vogel |
| 12. J. O. Johnson | 33. RRD Document Control Center |
| 13. R. A. Lillie | 34. ORNL Laboratory Records |

EXTERNAL DISTRIBUTION

35. Lap-Yan Cheng, Mail Stop 475B, Brookhaven National Laboratory, Upton, New York 11973-5000
36. M. Huttmaker, Office of Nuclear Energy, NE-40-GTN, Department of Energy, Germantown, MD 20874-1290
37. Dr. D. Kutikkad, University of Missouri Research Reactor Facility, Columbia, Missouri 65211
38. Dr. J. C. McKibben, University of Missouri Research Reactor Facility, Columbia, Missouri 65211
39. G. J. Malosh, ORNL Site Office, Department of Energy, Oak Ridge National Laboratory, Oak Ridge, Tennessee 37831-6269
40. J. O. Moore, ORNL Site Office, Department of Energy, Oak Ridge National Laboratory, Oak Ridge, Tennessee 37831-6269
41. L. A. Smith, Nuclear Fuels Department, Entergy Services, Inc., 1340 Echelon Parkway, Jackson, Mississippi 39213
42. Dr. R. E. Williams, NIST Center for Neutron Research, 100 Bureau Drive, Stop 8560, Gaithersburg, MD 20899